

This file is part of the following reference:

Costen, Andrew Richard (1996) *The sedimentary, hydrodynamic and turbidity regimes at inner shelf coral reefs, Halifax Bay, Central Great Barrier Reef, Australia.* Honours thesis, James Cook University.

Access to this file is available from:

<http://eprints.jcu.edu.au/22882>

The author has certified to JCU that they have made a reasonable effort to gain permission and acknowledge the owner of any third party copyright material included in this document. If you believe that this is not the case, please contact ResearchOnline@jcu.edu.au and quote <http://eprints.jcu.edu.au/22882>

Chapter 5. Seismic and Vibrocore Stratigraphy

5.1. Seismic Stratigraphy

Turbid water conditions and variations in light attenuation are generally caused by resuspension of the clay- and silt-sized fractions of the surficial inner-shelf sediments of southern Halifax Bay. To determine sedimentary regimes (present and past) it is essential that the presence or absence of these fractions be identified near Paluma Shoals and Phillips Reef, along with their vertical and lateral extents. Therefore, identification of the vertical and lateral variation in sediment types is essential for the correct interpretation of turbidity data.

The University research vessel *James Kirby* was used to collect 79 km (43 nautical miles) of high-resolution seismic images during leg-2 of cruise KG954 (Figure 5.1 & Appendix 5.1). Eight seismic facies have been identified within the inner-shelf of southern Halifax Bay (Table 5.1). A schematic cross-shelf section (Figure 5.2) illustrates the typical distribution of these facies within the study area. The identification of the individual seismic facies is based upon external form, spatial relationships and internal structure (Table 5.1). Vibrocore data (detailed below) and surficial sediment samples collected during leg-3 and leg-1 of cruise KG954 have been used to ground-truth the seismic profiles. The thickness of the seismic units has been determined, the depth to reflector A (Figure 5.2B) resolved and all bed elevations are given in metres below AHD.

5.2 Description and Interpretation of Seismic Facies

The descriptions of the seismic facies are largely consistent with previous investigations of the shallow seismic stratigraphy of the central GBR inner-shelf region. Previous investigations include Johnson *et al.* (1982) Johnson & Searle (1984) Tye, (1992) Carter *et al.* (1993) and Toohey (1994).

Of the eight facies identified, four are considered post-glacial, two are inferred as Pleistocene to early post-glacial and two are Pleistocene deposits. A bay-wide, shallow, laterally extensive subsurface reflector has been identified as Reflector A (as defined by Johnson *et al.*, 1982).

Seismic Facies	T ₄	Ch ₂	Ch ₁	Ch ₃	T ₃	T ₂	T ₁	P ₁
Thickness	Max acoustic penetration ~10 m AHD	Max 13 m	Max 17 m	Max 4 m	Max 3.5 m	Max 2.5 m	Max 1.6 m	Max 14m-Phillips Reef. 5 m Paluma Shoals
Lateral extent	> 11km	Max width 600 m	Max 900 m	Max width 150 m	Max width 900 m	Visible on all profiles	Visible on all profiles	Phillips 400 m max Paluma Shoals max ~400 m
Morphology	Tabular, deeply incised upto -27 m AHD	Complex patchy channel fill	Draped channel fill	Massive channel fill	Mound above channel.	Tabular over short distances/ sheet	Sheet/flat-topped thins in both a shoreward and seaward direction	Irregular, steep-sided flats (Paluma Shoal) & mounds (Phillips reef)
Internal structure	Weak parallel reflectors or acoustically transparent	Multiple patchy semi-continuous channel reflectors	Multiple continuous/ semi-continuous irregular layered	Acoustically transparent	Acoustically transparent	Acoustically transparent	Acoustically transparent occasional dark fuzzy patches	Semi-prolonged continuous-opaque
Location	Ubiquitous	Localised to channels.	Localised to channels.	Localised to channels.	Localised to one channel (Figure 4.8)	Widespread, fills topography	Widespread	Coral reefs
Relationship	Underlies all post-glacial units. Reflector A forms upper surface	Infills channels incised into T ₄ overlies Ch ₁ , overlain by Ch ₃ , T ₃ , T ₂ & T ₁	Infills channels incised into T ₄ overlies Ch ₂ overlain by T ₃ , T ₂ & T ₁	Infills channels incised in T ₂ & T ₄ -overlies Ch ₁ & Ch ₂ , overlain by T ₁ and T ₂	Overlies Ch ₁ & Ch ₂ .	Can be laterally continuous with Ch ₃ or overlies it, overlies Ch ₂ , Ch ₁ and T ₄	Overlies all other postglacial units	Overlies T ₄
Interpretation	Fluvial dominated sub-aerial deposit	Fluvial channel deposits	Episodic fluvial & estuarine channel fill	Estuarine channel fill	Relict delta-front deposit	Estuarine	Modern coastal deposit	Modern reef growth
Example		Figure 4.5	Figure 4.6	Figures 4.6 & 4.7	Figs 4.8	Figure 4.7	Figure 4.7	Figures 4.3 & 4.4
Inferred age	Pleistocene	Pleistocene	18 ky to 8.5 ky	8.5 ky to 6.5 ky	18 ky to 8.5 ky	8.5 ky to 6.5 ky	8.5 ky to 6.5 ky	8.2 ky to present

Table 5.1 *Characteristics of seismic facies from southern Halifax Bay.*

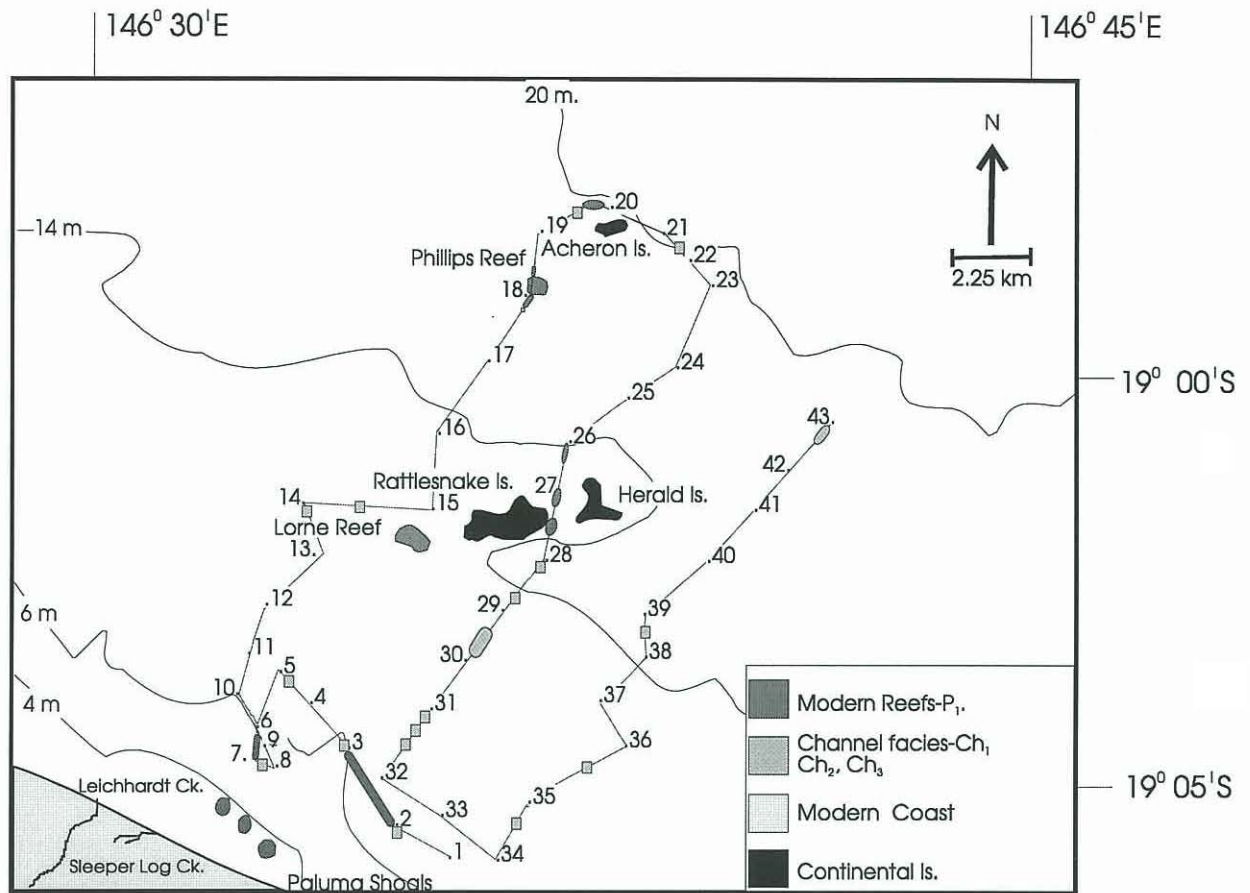


Figure 5.1. Location of seismic stations and track lines and the distribution of seismic facies Ch_1 , Ch_2 , Ch_3 and P_1 .

Reflector A

Reflector A is defined as the first lithological non-marine to marine disconformity intersected beneath marine post-glacial sediments (Orme, 1978; Davies *et al.*, 1981; Johnson & Searle, 1984; Cater *et al.*, 1993). Johnson *et al.* (1982) noted that Reflector A is the shallowest prominent sub-bottom reflector of regional extent throughout the central Great Barrier Reef region. Reflector A is characterized by an irregular incised surface and represents the last major shelf-wide sedimentary change.

Within the study area Reflector A is identified as a strong, irregular reflector, sub-parallel to the modern sea floor and commonly incised by channels (Figures 5.3 to 5.8). Across southern Halifax Bay, Reflector A has a gentle seaward gradient of 1.25 m/km, with structure contours parallel to the modern coastline (Figure 5.2B). This gradient is consistent with previous findings of Reflector A on the inner-shelf of the central GBR Province (Table 5.2).

Location	Slope	Source
Ingham	0.80 m/km	Johnson & Searle, 1984
Townsville	0.55 m/ km	Johnson & Searle, 1984
Bowen	1.78 m/km	Johnson & Searle, 1984
S Halifax Bay	1.02 m/km	Tve, 1992
N Halifax Bay	1.2 m/km	Tooev, 1994

Table 5.2. Gradients of Reflector A reported by previous studies.

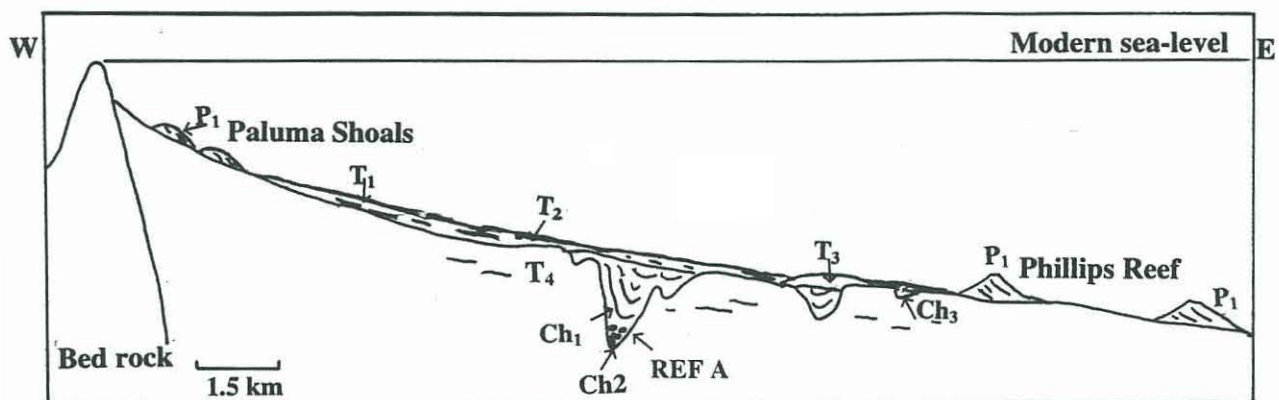


Figure 5.2. Schematic cross section of the distribution of eight seismic facies within southern Halifax Bay (modified from Johnson & Searle, 1984). Reflector A is incised by channels infilled with facies Ch_1 and Ch_2 . Facies T_2 drapes and fills the underlying topography and is incised by facies Ch_3 . All post-glacial and Pleistocene facies within southern Halifax Bay are overlain by facies T_1 which forms a thin bay-wide veneer of modern marine sediment. Facies T_3 forms a relict deltaic deposit above an abandoned or drowned channel. Facies P_1 forms modern reefs such as Paluma Shoals and Phillips Reef.

Reflector A has been identified and traced on all seismic profiles. Variations in depth of Reflector A below AHD range from approximately -10 m AHD close to the coast to -20 AHD seaward of Acheron Island (Figure 5.2B). Where incised by channels Reflector A can be as much as -27 m AHD (Figure 5.7). Reflector A is defined as the upper surface of facies T_4 .

Seismic Facies T_4

The upper surface of facies T_4 is defined by reflector A and is incised by numerous channels. Due to low penetration, the Pleistocene facies cannot be resolved in any detail. However, previous seismic data reveals that: 1) acoustically, T_4 is less transparent than

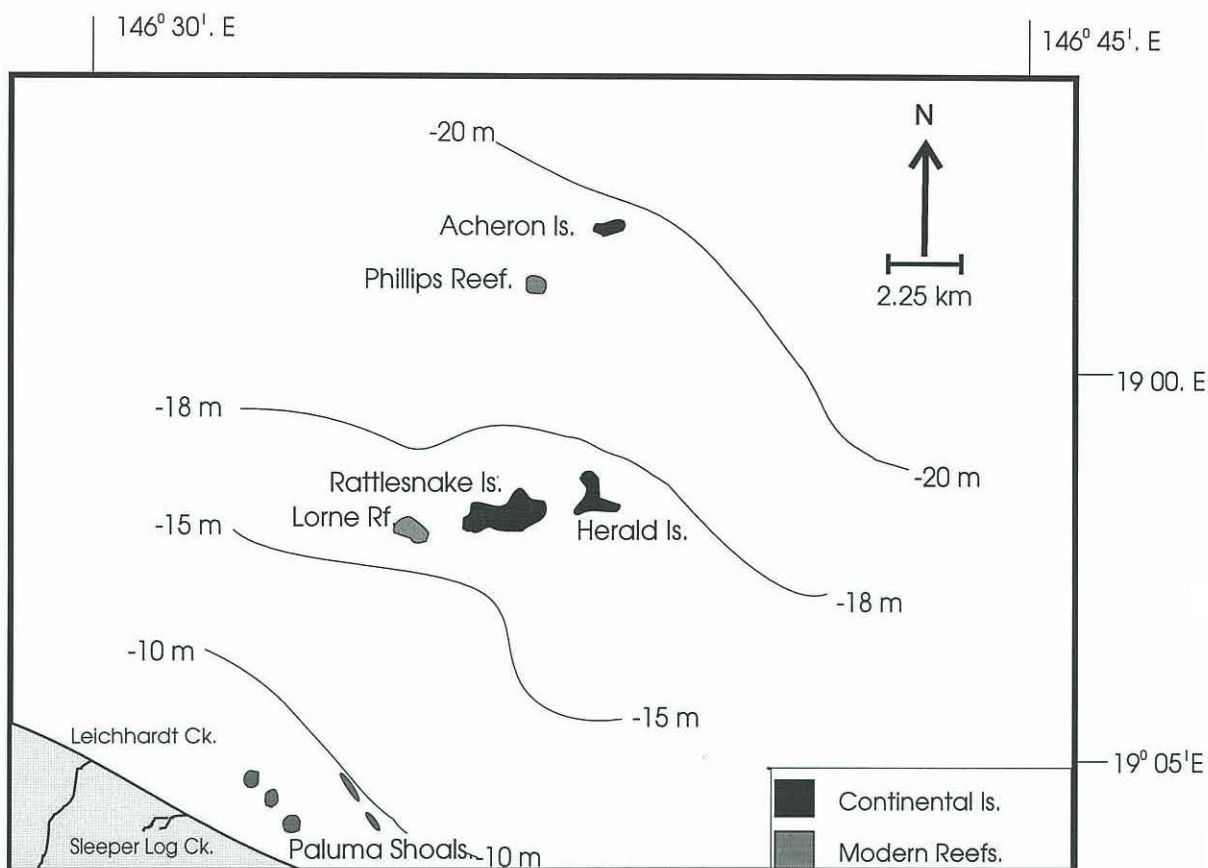


Figure 5.2b. Structure contour map of Reflector A interpreted from seismic profile data. Depths to Reflector A are in metres below AHD. Reflector A has a gentle seaward slope of 1.25 m/km.

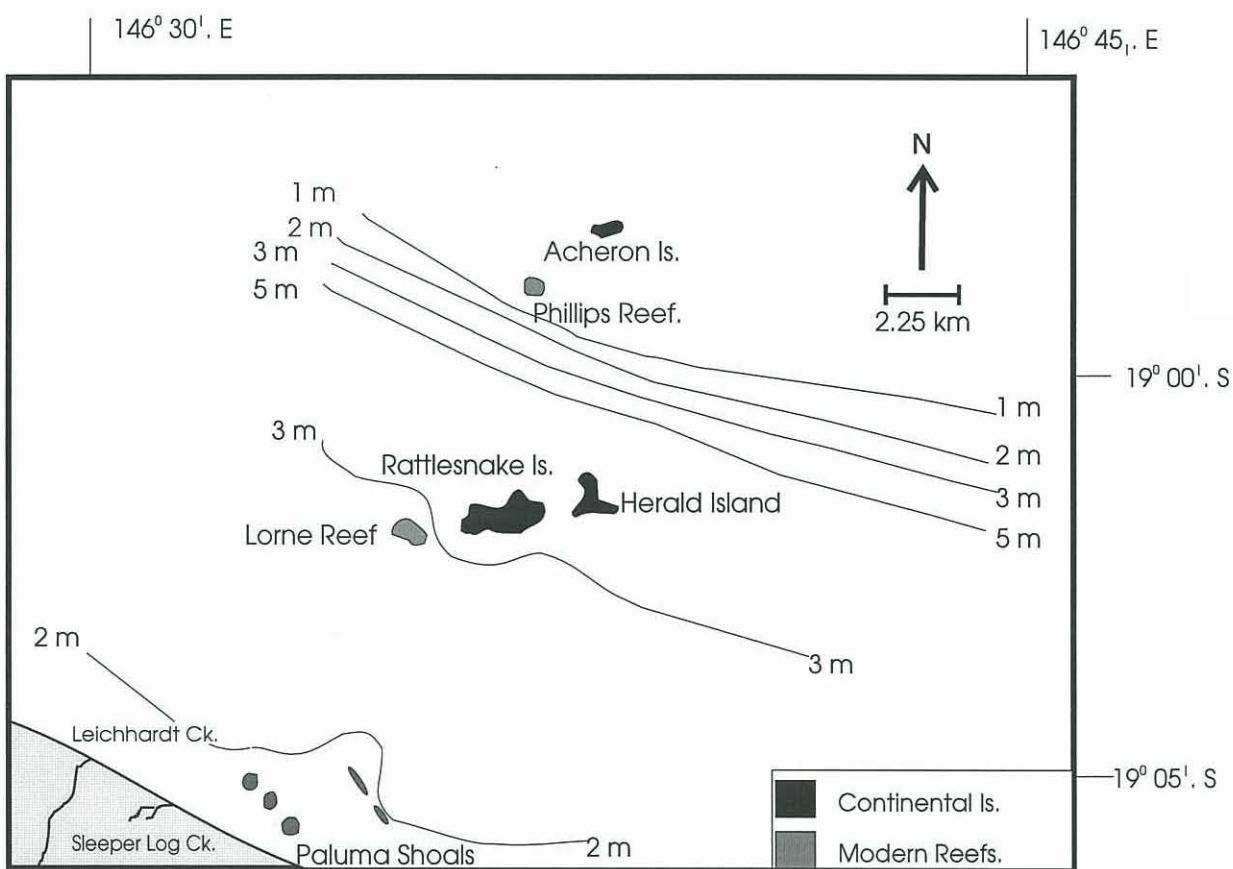


Figure 5.2c . Isopach map of seismic units T_1 and T_2 . Thickness of the combined units are in metres. Facies T_1 and T_2 thin in both a landward and seaward direction. North of Phillips Reef facies T_1 and T_2 are thin or absent.

overlying units and 2) internal structures vary from gently undulating and hummocky to parallel to sub-parallel internal reflectors (Johnson *et al.*, 1982; & Johnson & Searle, 1984).

Facies T₄ has been interpreted previously as the Pleistocene acoustic basement underlying all other Pleistocene and post-glacial sediments. Its upper surface is bound by a shallow seismic discontinuity, Reflector A. Previous investigations (Johnson *et al.*, 1982; Johnson and Searle, 1984 & Carter *et al.* (1993) have interpreted this unit as a fluvial dominated sub-aerial deposit, formed during the Pleistocene, glacial low stand. This interpretation is confirmed from shallow stratigraphic sections through the modern bay floor and the underlying late Pleistocene facies exposed during the 1985-86 Townsville Casino excavations (Carter *et al.*, 1993). The shallow stratigraphic sections indicate that the Pleistocene basement is comprised of deeply weathered clay containing carbonate and or Fe-Mn nodules, consistent with sub-aerial weathering in a tropical environment (Carter *et al.*, 1993).

Channel Deposits

Facies Ch₁, Ch₂ and Ch₃ form the fill of a regional channel system which is incised into facies T₂ and T₄. Previous investigations of facies that form channel fills in the incised Pleistocene surface have interpreted these units as fluvial and /or estuarine fill, deposited during sea-level rise and/or channel abandonment (Johnson & Searle, 1982; Johnson & Searle, 1984; & Toohey, 1994). Carter *et al.*, (1993) note that the channel fill deposits form a widespread channel system, incised part into what is defined as facies T₂ but mostly into the Pleistocene surface.

Attempts to map the extent of this 'shelf wide' channel system has resulted in reconstruction of Pleistocene palaeo-drainage patterns (Johnson *et al.*, 1982; Carter *et al.*, 1993 & Toohey, 1994). The reconstruction of these patterns is based on dense seismic coverage. However, attempts to trace single channels, even on the scale of the modern Burdekin River (Figure 5.6) do not reveal a continuous channel system, rather a sporadic pattern of incised channels. From this data, complex palaeo-drainage patterns have been reconstructed simply by joining the 'gaps' in the sedimentary record, producing a model of a shelf-wide meandering channel system (Carter *et al.*, 1993). The inability to trace these channel systems is a major hurdle when reconstructing the palaeo-drainage pattern.

The channel facies identified by this study are largely consistent with previous investigations. However, the precise interpretation of the facies identified in this and previous studies, requires deep coring of these channels to ground truth the seismic imagery.

Seismic Facies Ch₁

Acoustically facies Ch₁ is a multiple continuous/semi-continuous parallel to sub-parallel or truncated channelised facies (Figure 5.6). The facies displays irregular spacing and intensity of transparent and opaque internal reflectors. Unit Ch₁ commonly overlies Ch₂ and is overlain by T₂ and/or T₃ and T₁ (Figures 5.5 & 5.6).

The irregular spacing and the variations in intensity of reflectors within facies Ch₁ may represent bedding of coarse and fine material, possibly sand and muds (Figure 4.5). Carter *et al.* (1993) has interpreted similar parallel to sub-parallel features as fluvial point bars and the drape like features (Figure 5.6) as the infill of abandoned channels.

Seismic Facies Ch₂

Facies Ch₂ is a multiple, patchy, semi-continuous parallel to sub-parallel channelised facies. Facies Ch₂ commonly underlies facies Ch₁ and/or Ch₃ (Figure 4.5)

The stratigraphic position of facies Ch₂ (below Facies Ch₁ & Ch₃) and its patchy but strong reflective nature indicate that this facies may be a coarse channel fill. Facies Ch₂ are possibly gravel deposits, similar to the Pleistocene alluvial deposits along the modern coastline of southern Halifax Bay (Chapter 6.0).

Seismic Facies Ch₃

Facies Ch₃ is an acoustically transparent facies typically overlying Ch₁ and Ch₂. Facies Ch₃ commonly infills channels incising facies T₂. Ch₃ may occur as isolated channels (Figures 5.6 & 5.7) or as nested features above older and deeper channels incised into facies T₄ (Figure 5.4). Unit Ch₃ is commonly flanked or overlain by unit T₂.

Facies Ch₃ is interpreted as the fill of small tidal channels which were flanked by facies T₂. These channels may have been abandoned or drowned and backfilled during the Holocene transgression.

Seismic Facies T₂

Facies T₂ is an homogeneous acoustically transparent seismic facies that commonly drapes or fills the underlying topography of Reflector A. Facies T₂ is widespread, tabular over short distances and commonly flanks facies Ch₃ (Figure 5.7). Facies T₂ is difficult to distinguish seismically from the overlying T₁ facies.

The interpretation of this facies is aided by vibrocore data. Facies T₂ is interpreted as mangrove and/or coastal plain sediments deposited in the intertidal zones of southern Halifax Bay during the Holocene transgression ca. 8500 ybp. This interpretation is consistent with previous investigations (Tye, 1992; Carter *et al.*, 1993).

Seismic Facies T₃

Facies T₃ forms an acoustically transparent bathymetric high that disconformably overlies channel facies Ch₁ and Ch₂ (Figure 5.8).

The position and description of this facies is consistent with the interpretation of Johnson *et al.* (1982) and Johnson and Searle. (1984) as a relict delta front, deposited over backfilled channels during the transgression. Johnson and Searle (1984) attribute the scarcity of this facies to low sediment supply unable to produce mounds large enough to survive reworking during the transgression.

Seismic Facies T₁

Facies T₁ is a laterally extensive bay wide facies and has a gentle and uniformly seaward dipping surface. Facies T₁ is acoustically transparent with intermittent, reflective, dark fuzzy patches (Figure 5.7). Facies T₁ thins in both a shoreward and seaward direction (Figure 5.2C). In places, the thickness of unit T₁ is difficult to determine due to its weak internal reflectance and the absence of the reflective shoreline facies which is present in Cleveland Bay (Carter *et al.*, 1993; Ward *et al.*, 1995). The combined thickness of Facies T₁ and T₂ has been determined by vibrocore and seismic data. Facies T₁ and T₂ thin in both a landward and seaward direction (Figure 5.2c) and appear thin or absent NNE of Phillips Reef (Figure 5.4).

Vibrocore and grab sample data indicate that this facies is comprised of sandy muds and muddy sands, representing the modern marine depositional facies and forms a thin bay-wide veneer.

Facies P₁

Facies P₁ forms irregular steep-sided mounds and platforms rising sharply from the surrounding topography. It forms a prolonged continuous reflector with a slight hummocky or undulating surface (Figures 5.3 & 5.4). Near the coast, facies P₁ has formed 0.6 m high, 300 to 400 m long platforms or symmetrical mounds 10 m wide (Paluma Shoals) (Figure 5.2). Further offshore, P₁ forms a flat-topped (25 m) body (400 m-wide) rising 6.75 m above the surrounding sea bed (Phillips Reef) (Figure 5.4). Facies P₁ is interpreted as modern coral reef.

4.3 Vibrocores

A vibrocore program was undertaken in southern Halifax Bay to ground-truth the 3.5 KHz seismic profiles (leg-3 cruise KG954 24/10/95). A total of seven vibrocores were collected (Table 5.4 & Figure 5.9). The sedimentology of the subsurface sediments is described below and accompanied by a summary of the stratigraphy of each vibrocore. Photographs, descriptive logs, and data from grain size and carbonate analysis accompany the vibrocore descriptions (Figures 5.10-5.23). Detailed core logs and grain size results are presented in appendix 5.2 and 5.3 respectively.

The grain size data from the vibrocores was statistically grouped using Entropy 4.2 (Figure 5.24) (Woolfe & Michibayashi, 1995). These statistically derived groups closely match the sedimentary facies observed. The sedimentary facies defined within the vibrocores are based on a combination of grain size analysis, mineralogy and stratigraphy. A comparison between the statistically derived facies and those of more traditional methods can be observed in Figures 5.9 and 5.25. The Entropy groups are presented in Figure 6.25 and Appendix 6.3.

Core No	Latitude	Longitude	Water depth meters	Bed elevation (AHD)
KG954-VC1	19° 03.41' S	146° 33.30' E	11.25	-11.1
KG954-VC2	19° 04.00' S	146° 35.80' E	12.0	-12.6
KG954-VC3	19° 05.01' S	146° 37.61' E	11.25	-12.0
KG954VC3A	19° 05.01' S	146° 37.67' E	11.25	-12.0
KG954-VC4	19° 00.77' S	146° 41.55' E	17.25	-18.2
KG954-VC5	19° 00.70' S	146° 41.31' E	17.25	-18.2
KG954-VC6	19° 00.76' S	146° 41.81' E	17.25	-18.2

Table 5.4. *Vibrocore position, water depth (m) and bed elevation (AHD) data from leg 3 cruise KG954 24/10/95.*

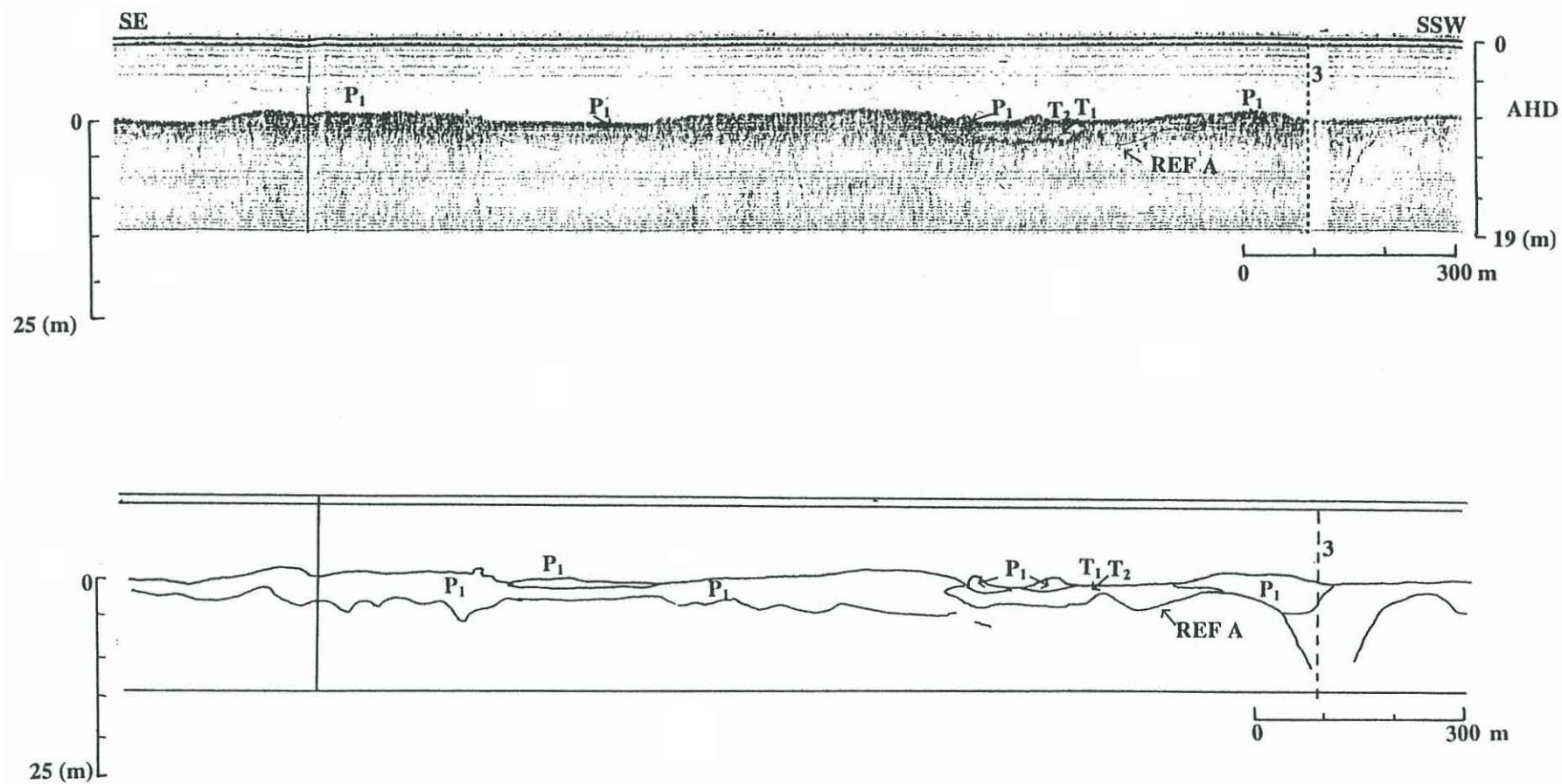


Figure 5.3 . Seismic profile between seismic stations 2 & 3. Reflector A (REF A) directly underlies facies P_1 (modern reef growth). Facies P_1 forms 0.6 m high, 300 to 400 m long platforms and bommie-like 10 m wide asymmetrical mounds.

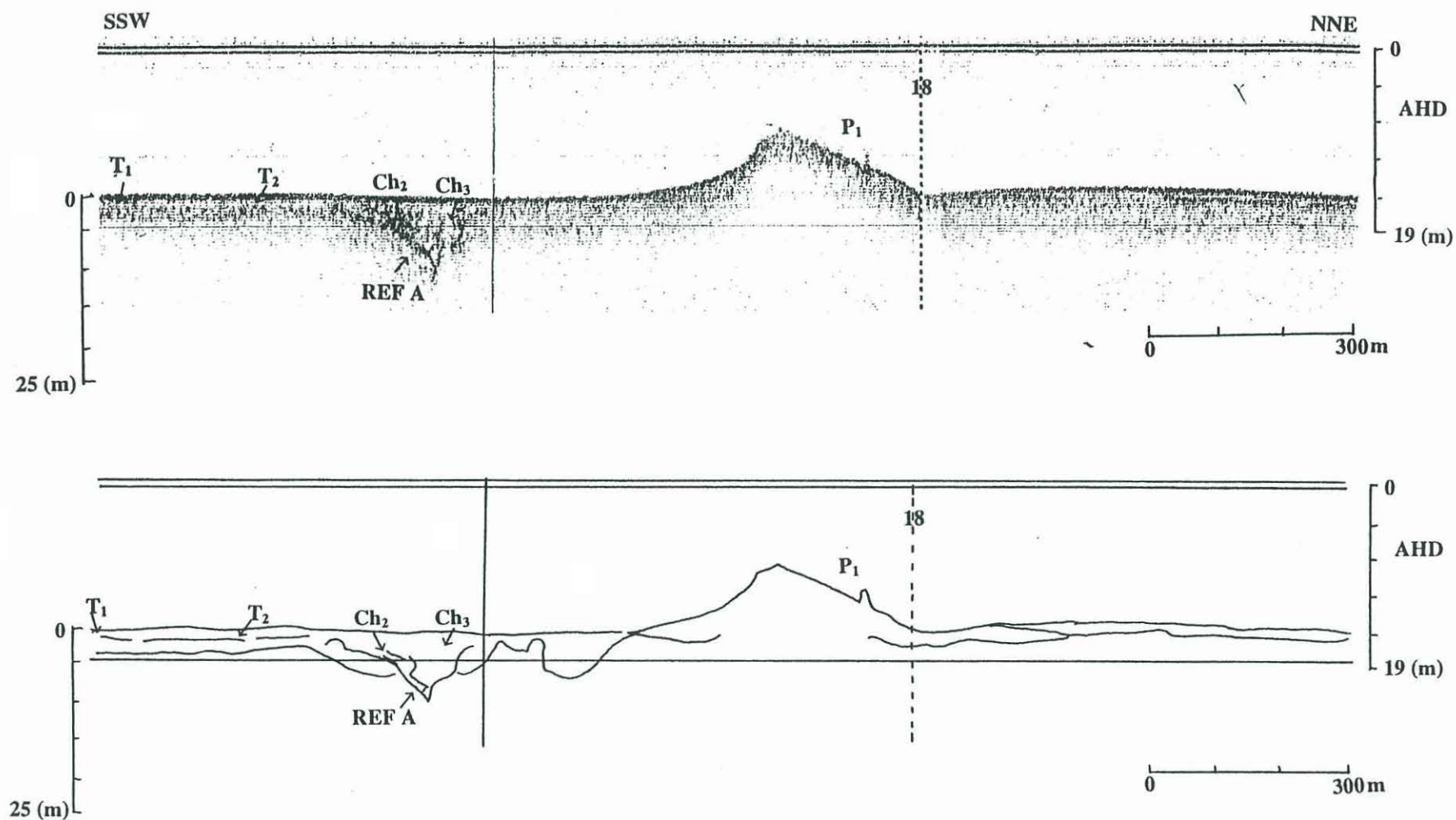


Figure 5.4. Seismic profile and line interpretation between seismic stations 17 and 18. The steep-sided, flat topped reflector is Phillips Reef (or part thereof). The reef slope on the SSW side is greater than the NNE slope and appears thicker, and may represent reef talus. Note that to Reflector A is incised by a channel infilled with facies Ch₂ and Ch₃.

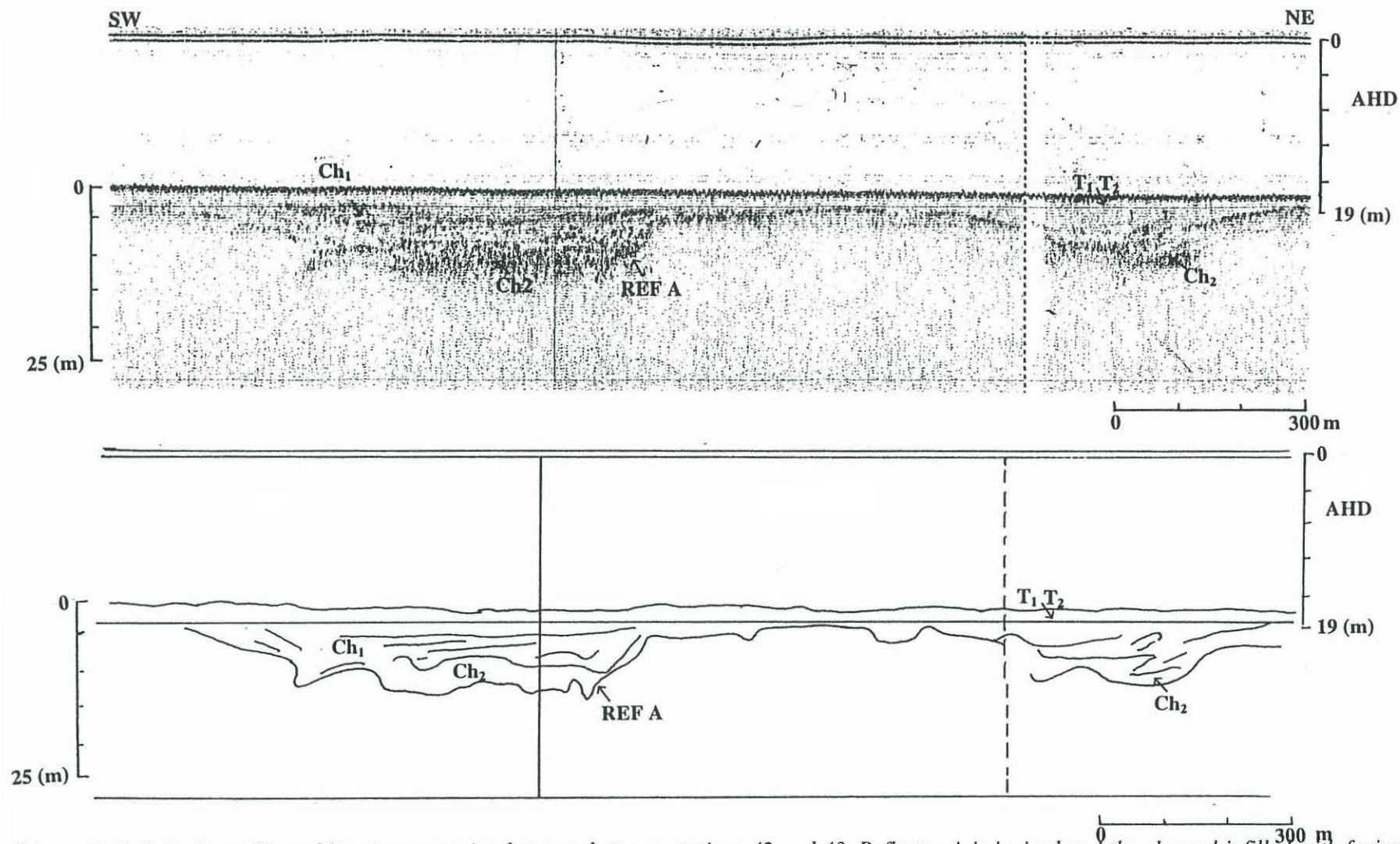


Figure 5.5. Seismic profile and line interpretation between stations 42 and 43. Reflector A is incised and the channel infilled with facies Ch_2 and Ch_1 . The opaque reflectors of Ch_2 are the result of strong attenuation of the seismic signal. These opaque patchy reflectors indicate that the fill comprising Ch_2 may be coarse. The overlying Ch_1 facies is comprised of parallel multiple reflectors, and have been interpreted as interbedded muds and sands, consistent with Carter et al. (1993).

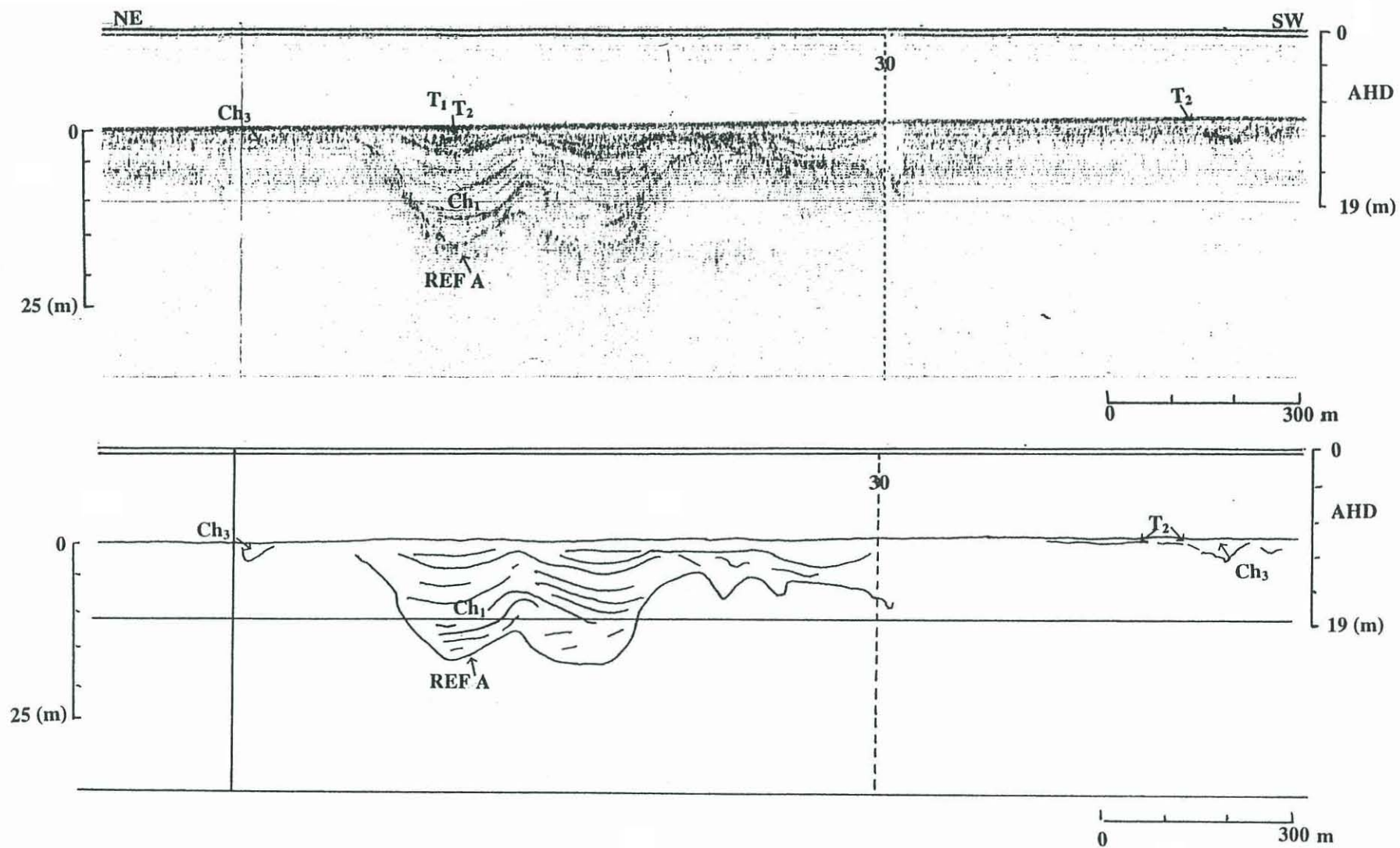


Figure 5. 6. Seismic profile and line interpretation between seismic stations 29 and 30. Reflector A is deeply incised (~ 27 m AHD) and infilled with channel facies Ch₁. Note how facies T₂ infills the topography above the channel facies. Facies T₂ flanks facies Ch₃ on the SW of the profile. Facies T₁ the modern bay fill forms a thin veneer (~1 m thick) over facies T₂.

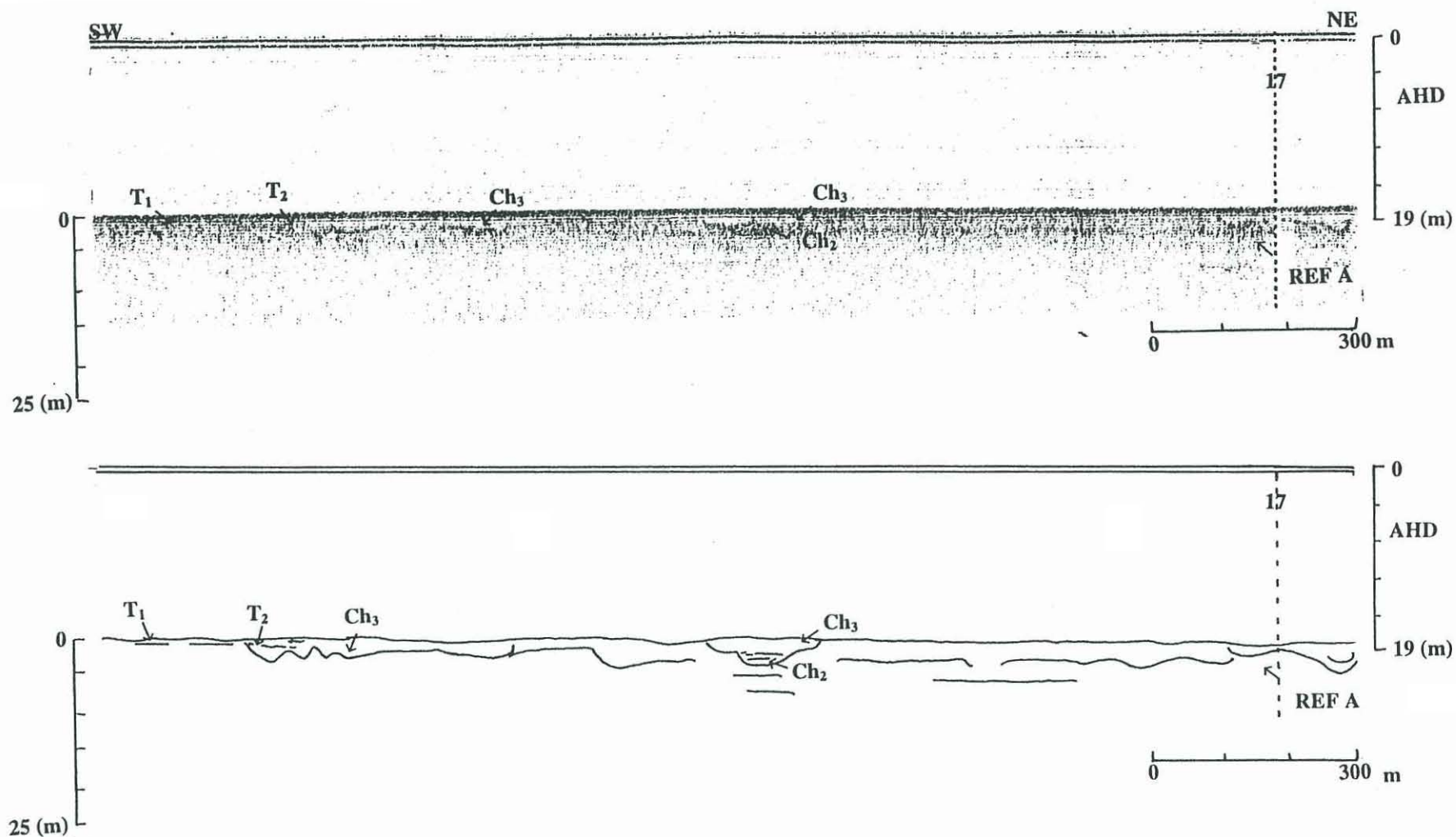


Figure 5. 7. Seismic profile and line interpretation between seismic stations 16 and 17. Facies Ch₂ infills the base of a 200 m wide channel (measured in a SW to NE direction) and is overlain by facies Ch₃. To the SW of the profile, facies Ch₃ forms the fill of isolated channels flanked by facies T₂. To the NE facies T₂ fills the underlying topography to a depth of ~ 3.5 m.

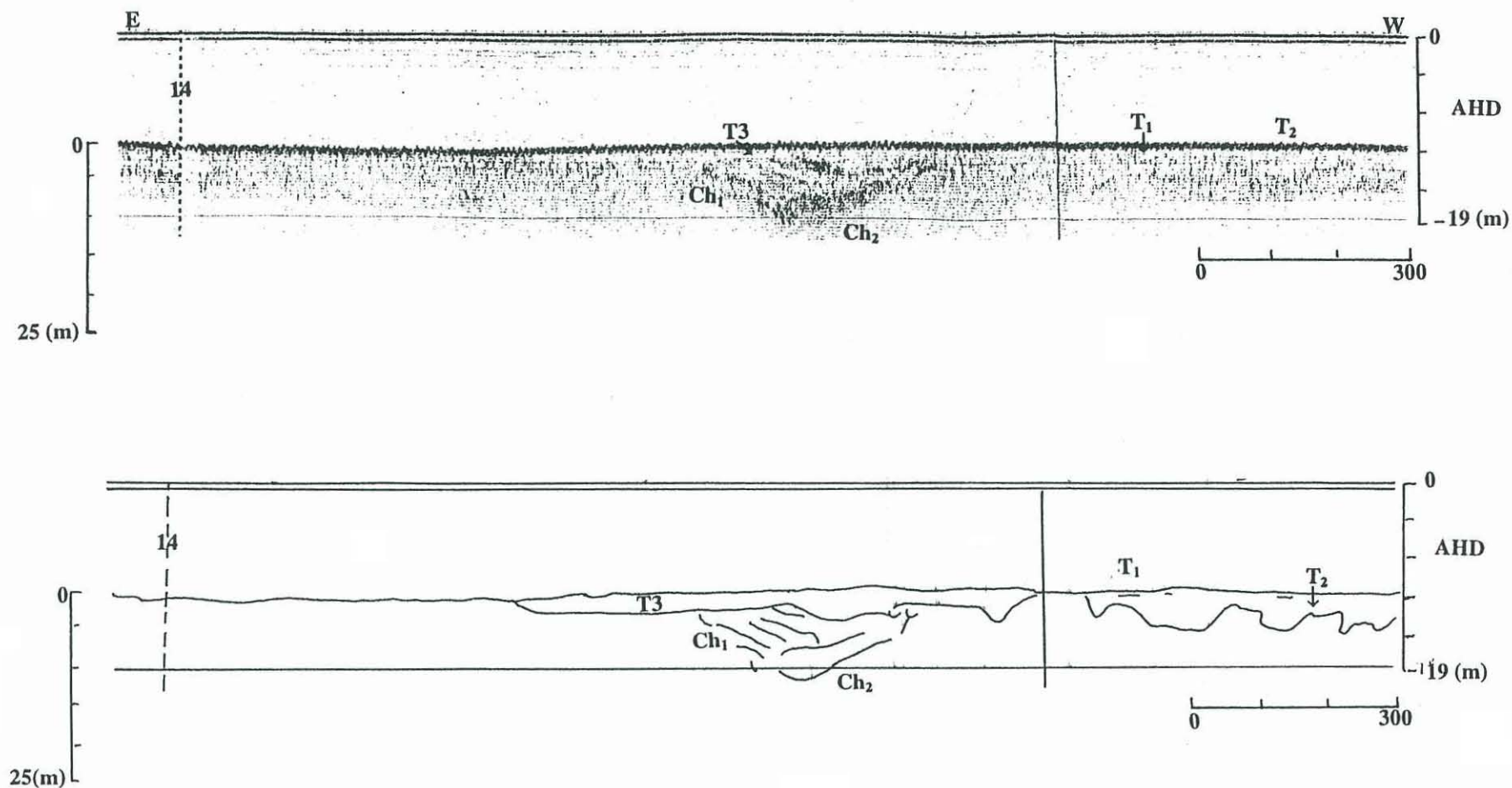


Figure 5. 8. Seismic profile and line interpretation between seismic stations 14 and 15. Facies T_3 forms the acoustically transparent bathymetric high that disconformably overlies channel facies Ch_1 . The mound is ca. 3.5 m thick at the centre and 900 m across as defined in an E-W direction. This facies is consistent with facies M1 of Johnson and Searle, (1984) and is interpreted as a relict delta front deposit. Channel facies Ch_1 appears truncated and overlies facies Ch_2 . Facies T_2 is forming the fill above Reflector A and is capped by facies T_1 the modern bay fill.

5.4. Vibrocore Facies Description and Interpretation

Four post-glacial facies have been identified on the basis of grain size, stratigraphic relationship and mineralogy:

Marine bay fill facies.

Mud flat facies.

Channel fill facies.

Mangrove facies.

Marine bay fill facies

Typically this facies is composed of olive grey, poorly sorted, bioturbated, gravelly, calcareous muddy sand and sandy mud. The facies exhibits a weak coarsening-upward trend and an increase in carbonate content, associated with the greater abundance of carbonate detritus near the surface. The upper 10-25 cm of this unit is paler and indicates oxidation of the sediment. The facies typically firms toward the base of the core

The facies has a trimodal sediment distribution pattern consistent with the bay fill facies from Cleveland Bay (Carter *et al.*, 1993). Tye (1992) hypothesised a scenario for this characteristic in Halifax Bay: terrigenous silts are deposited during low energy periods (mode 1) with high energy events such as storms, depositing layers of well-sorted quartose sand (mode 2) bioturbation of these sediments destroys the primary layering and adds the biogenic component to the sediment (mode 3). The inhomogeneous nature of the bay fill facies is the result of this cycle of deposition, bioturbation and winnowing. These sediments have accumulated under a similar regime to the modern marine sediments (Chapter 6).

The marine bay fill facies occurs in all vibrocores ranging in thickness from 0.56 m (VC3A) to 1.68 m (VC4). The facies overlies all other post-glacial sediments and is consistent with previous investigations of the modern bay fill facies (Tye, 1992; Carter *et al.*, 1993). Seismic data indicate that the facies thins in a landward and seaward direction.

Mud flat facies

Typically this facies is comprised of a dark grey (N3) massive, micaceous sandy mud with shell fragments and organic rich fine-grained lamina. The lamina are comprised of vegetable matter predominately coarser than 100 microns. The stratigraphic position of this facies and the absence of coalified wood and rootlets indicate that it may be a mud flat

deposit. This interpretation is consistent with those of Belperio (1983) and Tye (1992). The mud flat facies occurs in all cores except VC4 and VC6. The facies directly underlies the bay fill facies

Channel fill Facies

This facies occurs in vibrocores VC2 and VC4 which penetrated nested channels incised into seismic facies T₂. Typically it is comprised of a massive dark grey (N3) bioturbated sandy mud, interbedded with 1-30 mm thick layers of well sorted subangular to subrounded fine sand. The sand lamina are comprised of 90% well sorted subangular to subrounded quartz grains with minor feldspar, hornblende and mica.

The facies may represent abandoned channels. The cyclic nature of the layering could be related to deposition during spring tides, flooding and infilling the abandoned channel (Figure 5.12 & 5.13). The filling of these channels could also be the result of rapid backfilling by sediment as sea-level rose during the Holocene transgression.

Mangrove facies

The facies is comprised of a stiff, massive, dark grey (4 N4) mud with minor wood fragments (< 3 mm in diameter) and yellow-grey (5Y B/4) oxidized, muddy sand patches (Figures 5.12 & 5.13). This facies occurs in vibrocores VC2 and VC4 (Figures 5.13 & 5.19) and underlies the channel facies. Typically the contact between the mangrove facies and the channel facies is sharp.

Due to the stratigraphic position below the channel facies and its composition this facies is interpreted as a mangrove facies. This interpretation is consistent with previous investigations (Tye, 1992; & Carter *et al.*, 1993).

5.6. Vibrocore Descriptions

KG954-VC1 (Figures 5.10 & 5.11)

The vibrocore was recovered at 19° 03.41' S - 146° 33.30' E (Table 5.3) to ground truth the seismic profile between stations 12 and 13. The core recovered 2.3 m of sediment overlying a palaeo-channel. Two distinct units are recognised, the bay fill facies and the mud flat facies.

The upper 0.18 m of the bay fill unit is composed of a light olive grey (5 Y 6/1) loose, poorly sorted, heavily bioturbated, gravelly, calcareous sandy mud with numerous large

coral fragments up to 40 mm in diameter. The underlying portion of the bay fill unit (0.62 - 0.98 m) is comprised of an olive grey (5Y 4/1) poorly sorted, bioturbated shelly sandy mud. The bay fill facies exhibits a weak coarsening-upward trend and a increase in carbonate content, associated with the greater abundance of carbonate detritus near the surface (Figure 5.11). The facies firms toward the base. The contact between the bay fill and underlying tidal mud flat facies is sharp but irregular.

The mud flat facies (0.98 - 2.305 m) is comprised of a dark grey (N3) massive, micaceous, sandy mud with minor shell fragments and organic-rich lamina. The lamina consist of small wood fragments. Grain size analysis of the lamina (Figure 5.11, KG954-VC1-5) indicate that the material is coarser than 100 microns.

KG954-VC2 (Figures 5.12 & 5.13)

KG954-VC2 was recovered at 19° 04.00' S - 146° 35.80' E to ground truth the seismic profile taken between stations 29 to 30 (Figures 5.1 & 5.6). Four facies are recognized including the bay fill, mud flat, channel and mangrove facies. The upper 0.13 m of the bay fill facies is composed of a light olive grey (5Y 6/1) poorly sorted, shelly muddy sand. The underlying portion (0.13 - 0.94 m) is an olive grey (5Y 3/2) loose, poorly sorted, bioturbated, shelly muddy sand. The facies exhibits a weak coarsening-upward trend and a increase in carbonate content, associated with the greater abundance of carbonate detritus near the surface (Figure 5.13).

The contact between the mud flat facies and the bay fill is sharp but irregular. The tidal mudflat unit (1.00 - 1.20 m) is composed of a dark grey (N3) bioturbated, micaceous sandy mud with abundant skeletal material (KG954-VC2-4). The sand component consists of subangular to subrounded quartz grains with abundant mica. facies is devoid of wood and carbon fragments.

The contact between the tidal mud flat facies and the underlying channel facies is sharp and regular. The channel facies (1.20 - 2.21 m) consists of a massive dark grey, bioturbated (N3) sandy mud (KG954-VC-2-6), interbedded with 1-30 mm thick layers of well sorted subangular to subrounded fine sand (KG954-VC2-5).. The sand lamina are comprised of 90% well-sorted subangular to subrounded grains of quartz and minor feldspar, hornblende and mica. The sandy muds and sands (<80 mm in thickness) are interbedded with < 5 mm thick organic lamina comprised of wood fragments (< 100 microns) (Figures 5.12 & 5.13).

The contact between the tidal channel facies and the mangrove facies is sharp. The mangrove facies (2.21-2.80 m) is comprised of a stiff, massive, dark grey (N3) mud with minor wood fragments (< 3 mm in diameter) and yellow-grey (5Y B/4) oxidized, muddy sand patches (KG954-VC2-7).

KG954-VC3A (Figures 5.14 & 5.15)

KG954-VC3A was recovered from 19° 05.01' S - 146° 37.67' E to ground truth a seismic profile taken between stations 36 and 37. Two distinct facies have been identified, including the bay fill facies and the mud flat facies. The upper portion of the bay fill unit (0 - 0.17 m) is comprised of a light olive-grey (5Y 5/2) poorly sorted, bioturbated, gravely, shelly muddy sand (KG954-VC3A-1). This unit is separated from the underlying bay fill unit by a sharp erosional contact. The underlying bay fill facies (0.17 - 0.58 m) is comprised of an olive grey (5Y 4/1) poorly sorted, bioturbated, shelly muddy sand. The bay fill facies exhibits a weak coarsening-upward trend and an increase in carbonate content, associated with the greater abundance of carbonate detritus near the surface (Figure 5.15).

The contact between the bay fill and the supratidal mud flat facies is scoured (Figure 5.15). The underlying unit (0.58 - 0.66 m) is comprised of a dark grey (5Y 8/4) sandy mud with patches of yellow-grey (5Y B/4) oxidized muddy sand. The sand fraction contains subangular to subrounded quartz grains with abundant mica. The facies is devoid of wood and carbon fragments.

KG954-VC3 (Figures 5.16 & 5.17)

KG954-VC3 was recovered from 19° 05. 01' S - 146° 37.61' E to ground truth the seismic profile between stations 36 and 37. Two facies have been identified, including the bay fill facies and the mangrove facies. The bay fill facies (0 - 0.88 m) is comprised of a moderate- brown (5Y 4/4) poorly sorted, shelly muddy sand (KG954-VC3-1). The facies exhibits a weak coarsening-upward trend and a increase in carbonate content, associated with the greater abundance of carbonate detritus near the surface. The unit darkens in colour toward the base (Figure 4.17). The contact between the bay fill facies and the underlying mud flat facies is gradational with the top 0.1 m of the facies heavily bioturbated. The facies is comprised of a dark grey (5Y 8/4) sandy mud (KG954-VC3-A) with patches of yellow-grey (5Y B/4) oxidized muddy sand. The sand fraction contains subangular to subrounded quartz grains with abundant mica. The unit is devoid of wood and carbon fragments.

KG954-VC4 (Figure 5.18 & 5.19)

KG954-VC4 was recovered from 19° 00.77' S - 146° 41.55' E to ground truth a seismic profile taken between stations 42 and 43. Three facies have been identified and include the bay fill, channel and mangrove facies. The top 0.15 m of the bay fill facies is comprised of a light olive-grey (5Y 6/1) poorly sorted, bioturbated, shelly muddy sand (KG954-VC4-1) with a sharp erosive contact at 0.15 m. The underlying component of the bay fill facies (0.15-1.68 m) consists of an olive-grey (5Y 4/1) poorly sorted, bioturbated, shelly muddy sand. The base of the facies is marked by an irregular, sharp contact. The bay fill facies exhibits a weak coarsening-upward trend and an increase in carbonate content, associated with the greater abundance of carbonate detritus near the surface.

The channel facies (1.68-2.90 m) is comprised of a dark-grey (N/3) sandy mud, interbedded with 1-30 mm thick layers of well sorted, subangular to subrounded fine sand. The sand laminae are comprised of 90% well-sorted subangular to subrounded quartz grains with lithics of feldspar, hornblende and mica. The sandy mud contains several small wood fragments up to 20 mm in diameter. The contact between the intertidal channel facies and the underlying mangrove facies is sharp and regular.

The mangrove facies (2.90-3.18 m) is comprised of a dark grey (N 3) stiff, massive slightly sandy mud (KG954-VC4-2). The unit contains abundant wood and carbon fragments and small (10-20 mm) yellow-grey (5Y 8/4) patches of muddy sand.

KG954-VC5 (Figure 5.20 & 5.21)

KG954-VC5 was recovered from 19° 00.70' S - 146° 41.81' E to ground truth the seismic profile taken between stations 42 and 43. The core penetrated 1.12 m of sediment, and two facies are identified, including the bay fill and the mud flat facies. The upper 0.20 m of the bay fill facies is comprised of a light olive grey (5Y 6/1) poorly sorted, bioturbated, shelly muddy sand (KG954-VC5-1). A sharp irregular contact separates the remaining 0.80 m of the bay fill unit which darkens toward the base and is comprised of an olive grey (5Y 4/1) poorly sorted, shelly muddy sand (KG954-VC5-2).

The contact between the overlaying bay fill and the mud flat facies is gradational and heavily bioturbated. The facies (1.0-1.12 m) is comprised of a dark grey (5Y 8/4) sandy mud (KG954-VC5-3). The sand component contains subangular to subrounded quartz grains with abundant mica. The unit is devoid of wood and carbon fragments.

KG954-VC6 (Figures 4.22 & 4.23)

KG954-VC6 was recovered from $19^{\circ} 00.76' \text{ S}$ - $146^{\circ} 41.81' \text{ E}$ to ground truth a seismic profile taken between stations 42 and 43. One facies has been identified. The bay fill facies is comprised of a light olive-grey (5Y 5/2) poorly sorted, bioturbated, gravelly shelly muddy sand (KG954-VC61-7). The carbonate content increases with depth, and the facies darkens and hardens toward the base of the core.

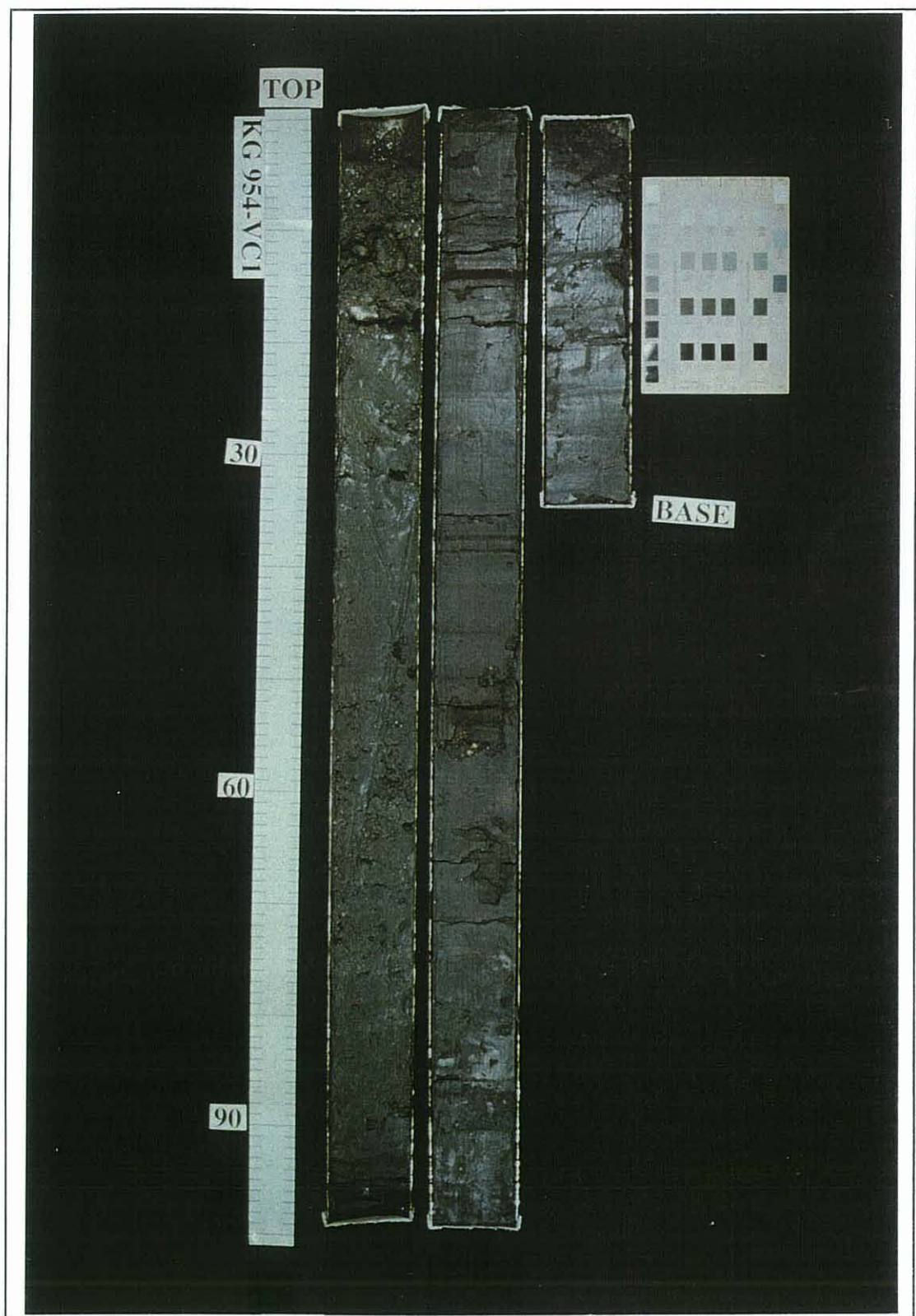


Figure 5.10. *Vibrocore KG954-VC1. Facies include the bay fill facies (0 - 0.98m) and the mud flat facies (0.98 - 2.305 m)*

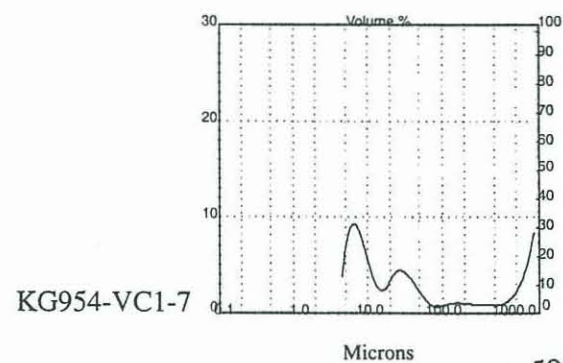
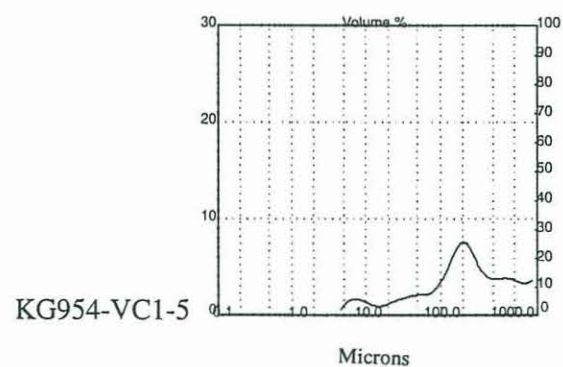
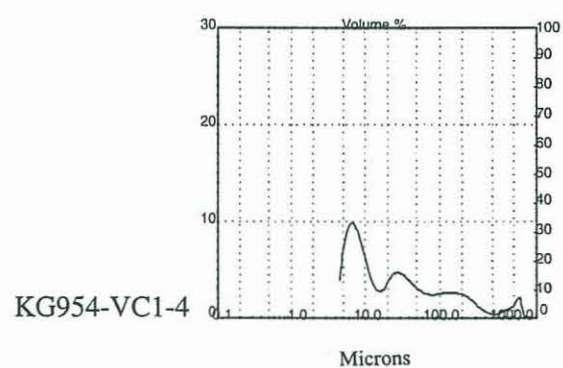
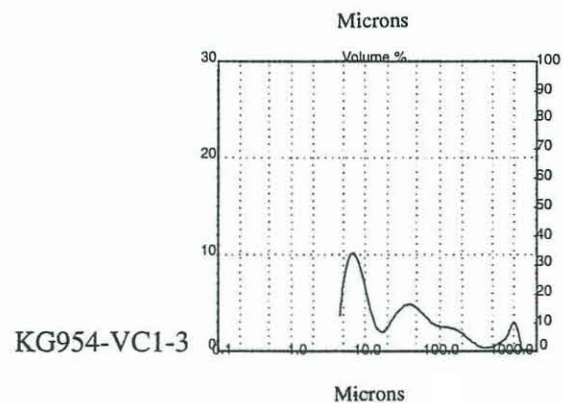
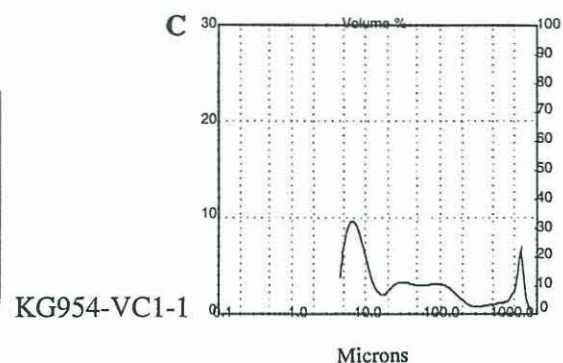
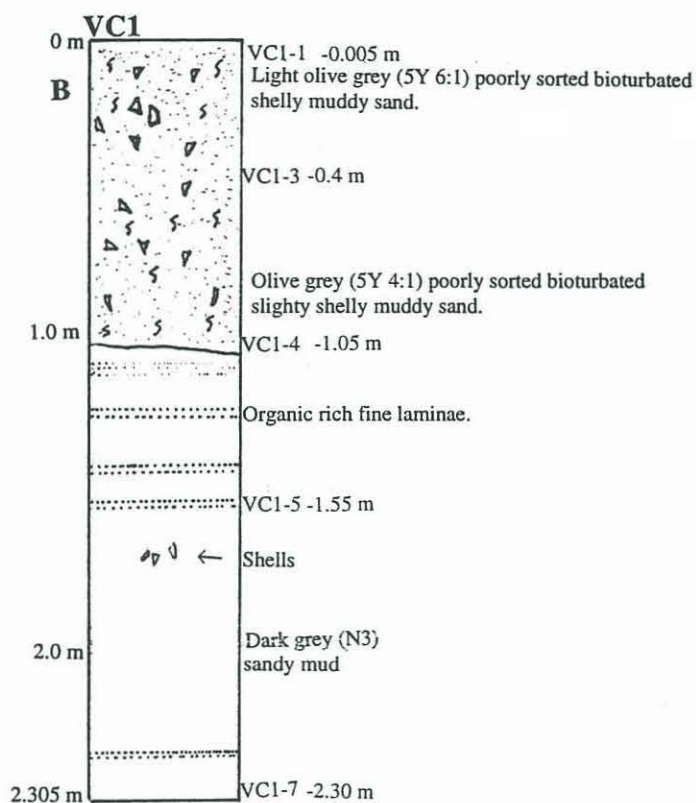
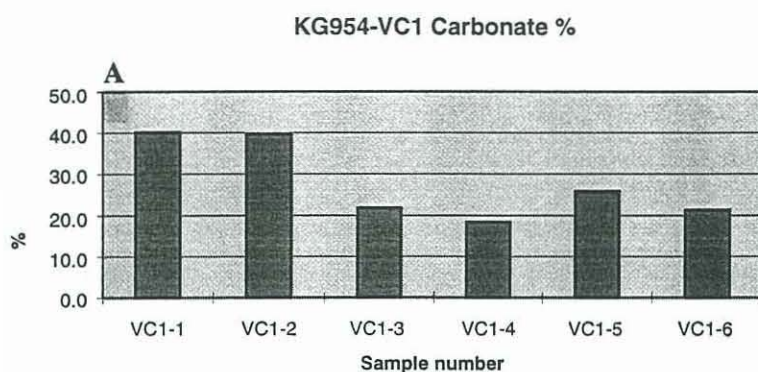


Figure 5.11. Data summary of vibrocore VC1 including: A) Graph of carbonate %; B) Vibrocore summary log of VC1; C) Grain size distribution of samples from VC1.

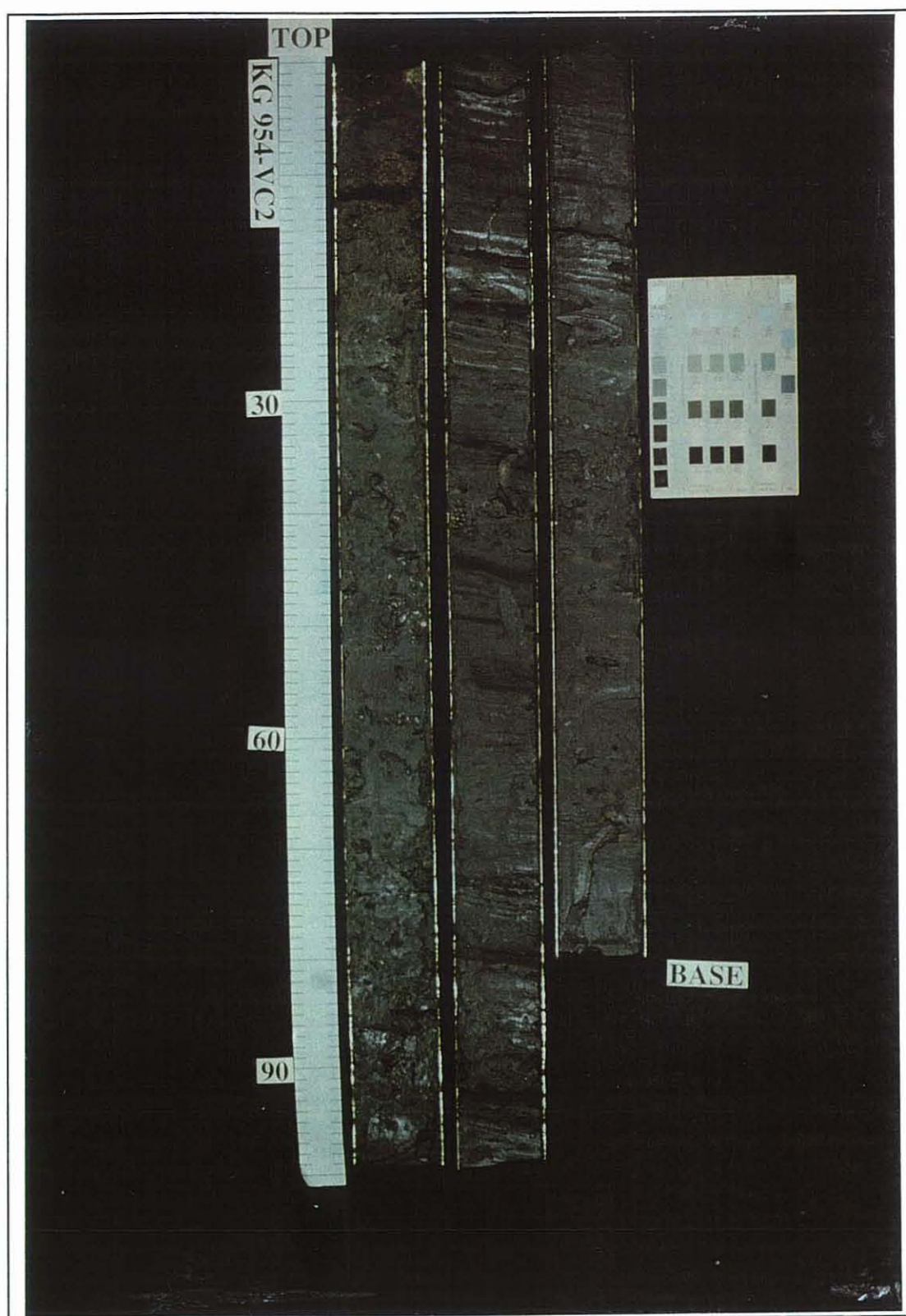


Figure 5.12. Vibrocore KG954-VC2. Facies include the bay fill facies (0-1.0 m) mud flat facies (1-1.20 m) channel facies (1.20 -2.21 m) and the mangrove facies (2.21 -2.80 m).

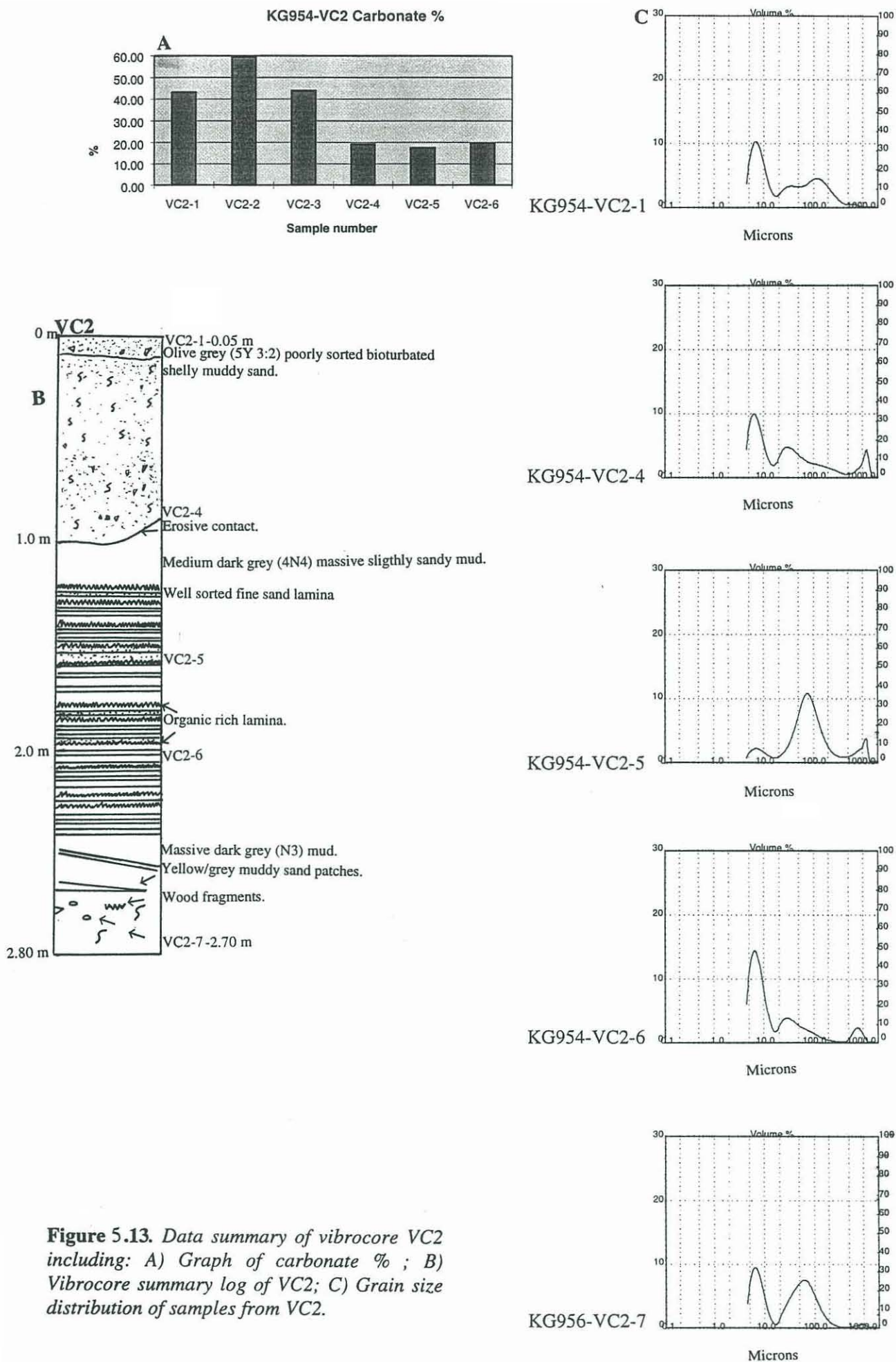


Figure 5.13. Data summary of vibrocore VC2 including: A) Graph of carbonate % ; B) Vibrocore summary log of VC2; C) Grain size distribution of samples from VC2.

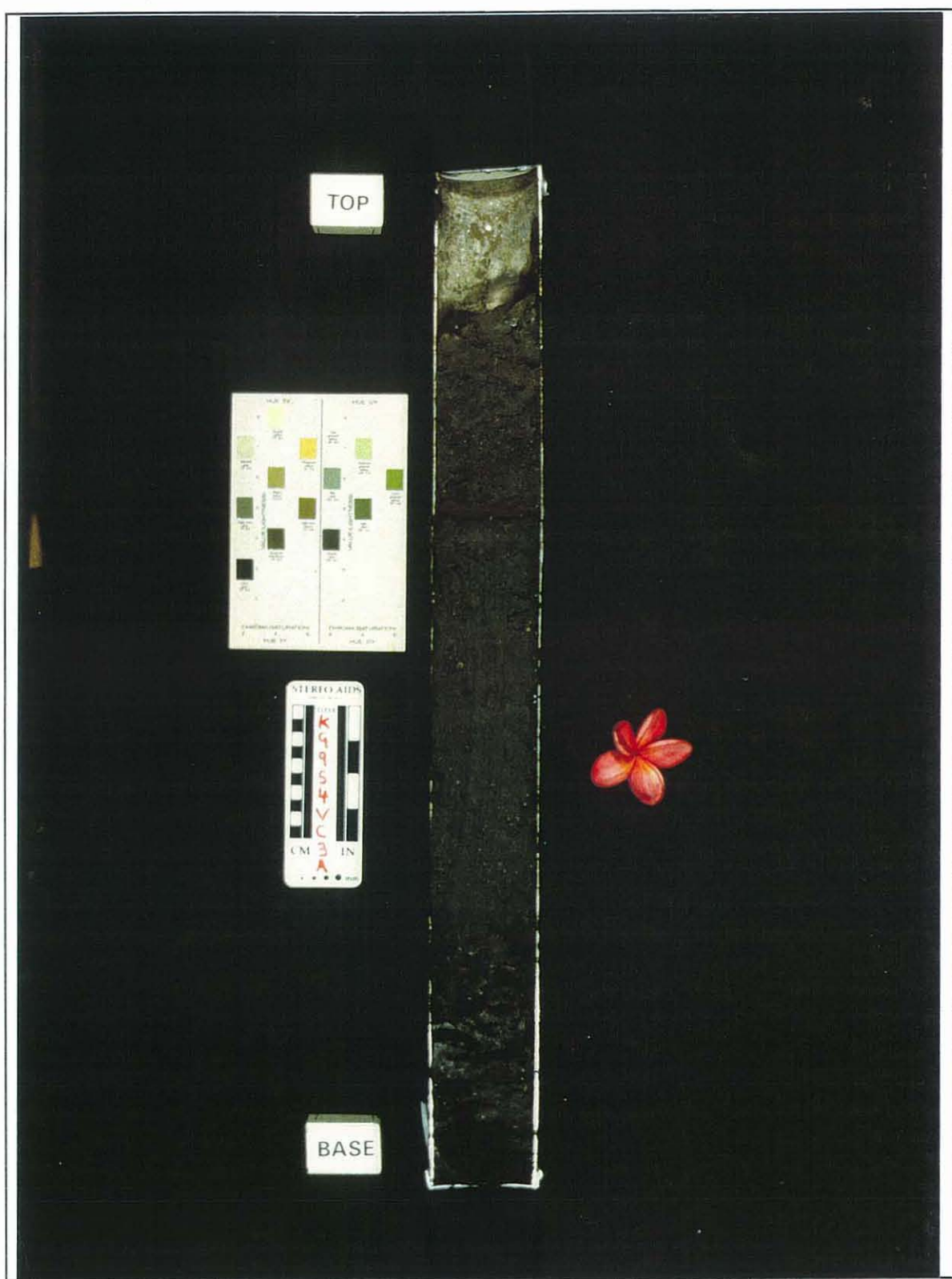
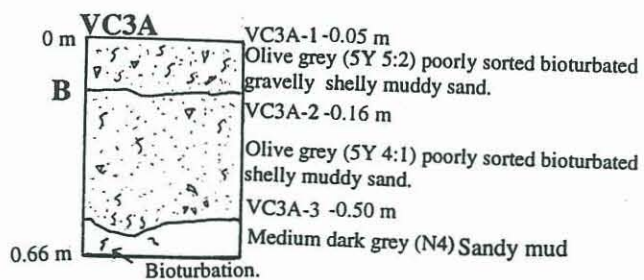
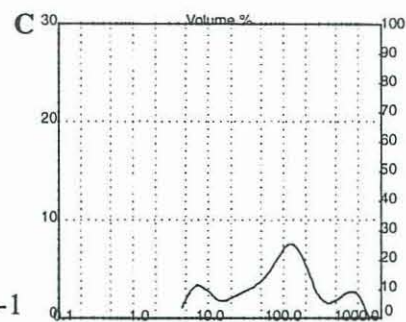


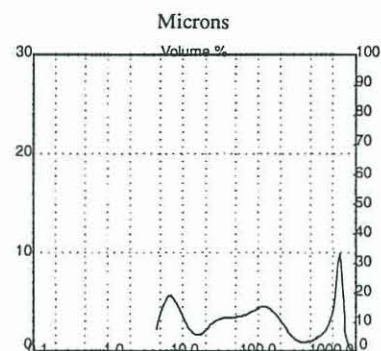
Figure 5.14. Vibrocore KG954-VC3A. Facies include the bay fill (0-0.58 m) and the mud flat facies (0.58-0.66 m).



KG954-VC3A-1



KG954-VC3A-2



KG954-VC3A-3

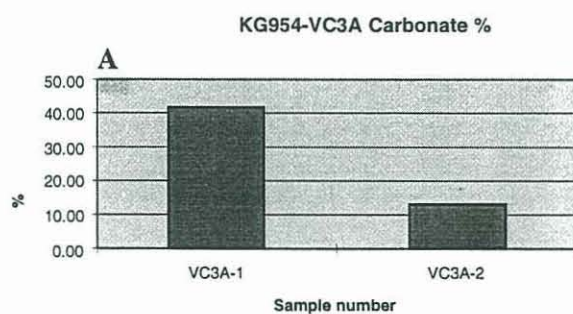
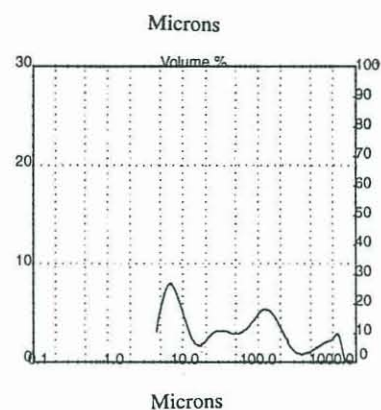


Figure 5.15. Data summary of vibrocore VC3A including: A) Graph of carbonate %; B) Vibrocore summary log of VC3A; C) Grain size distribution of samples from VC3A.

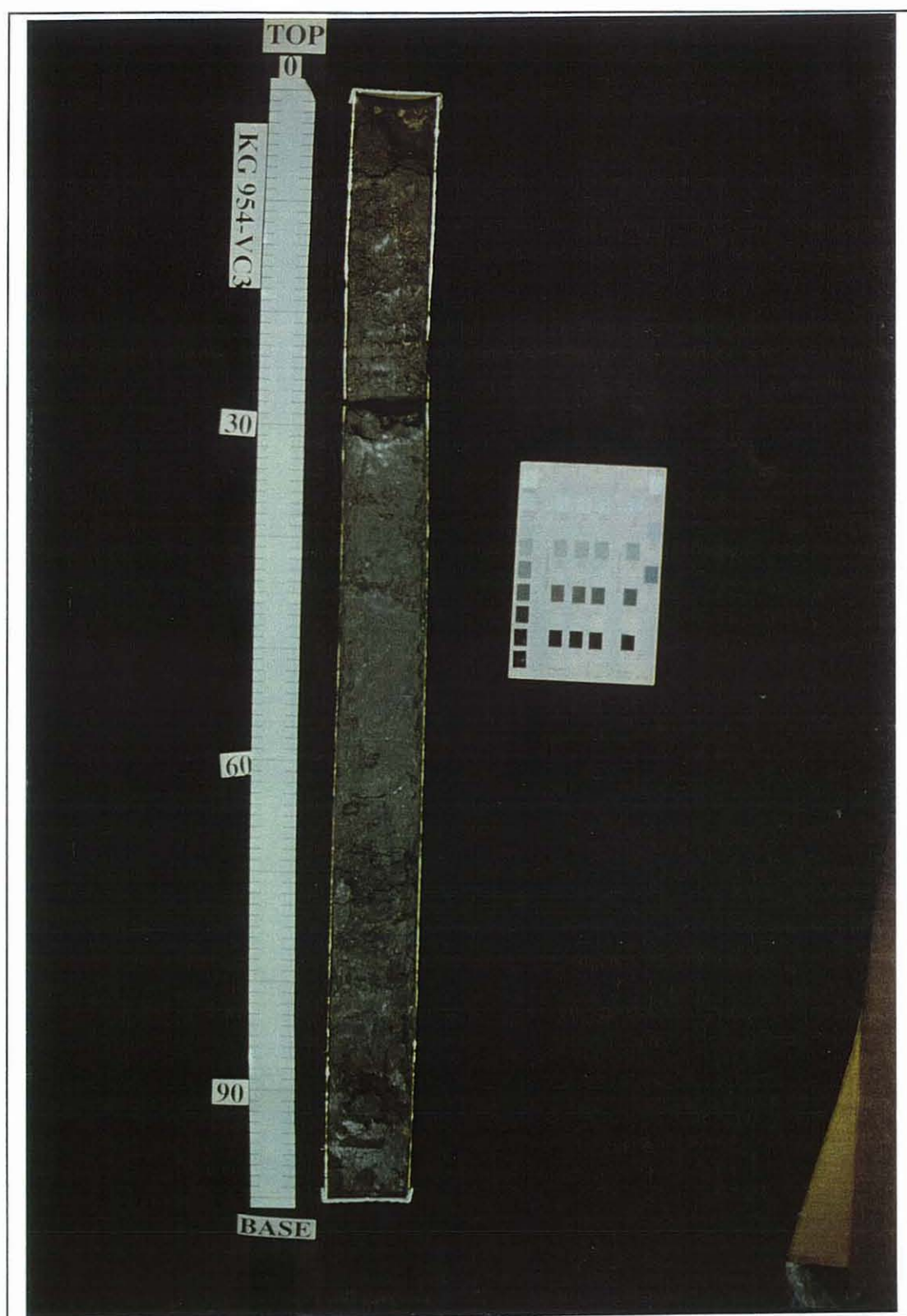


Figure 5.16. Vibrocore KG954-VC3. Facies include the bay fill (0-0.88m) and the mud flat facies (0.88-0.98 m).

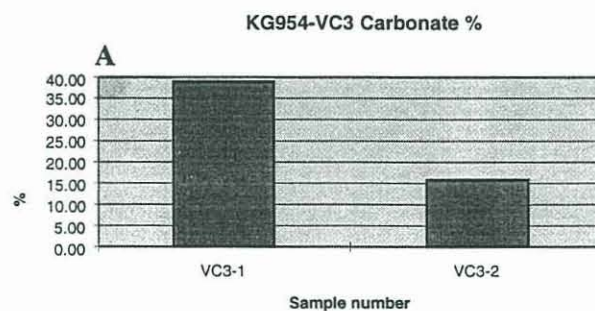
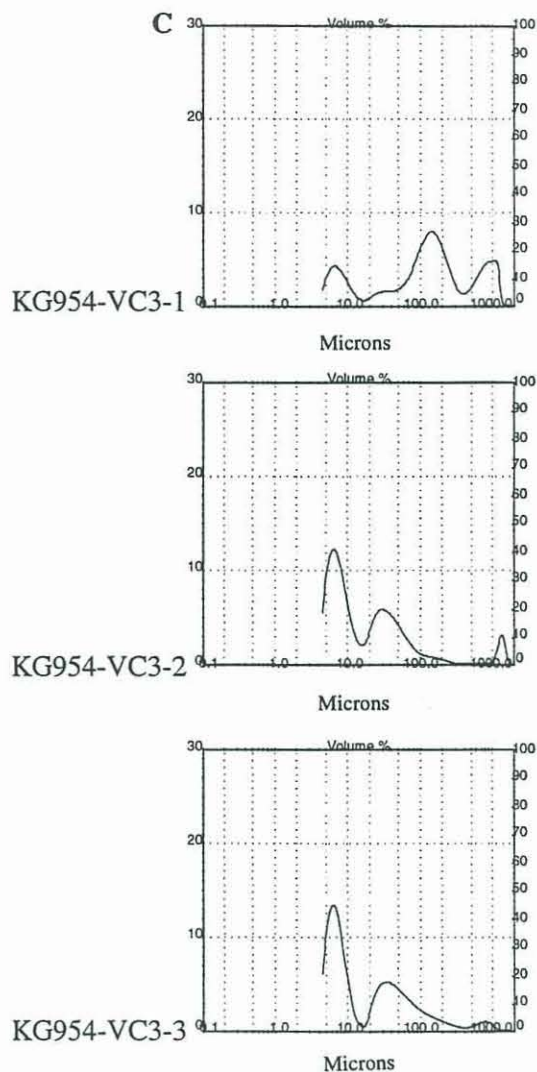
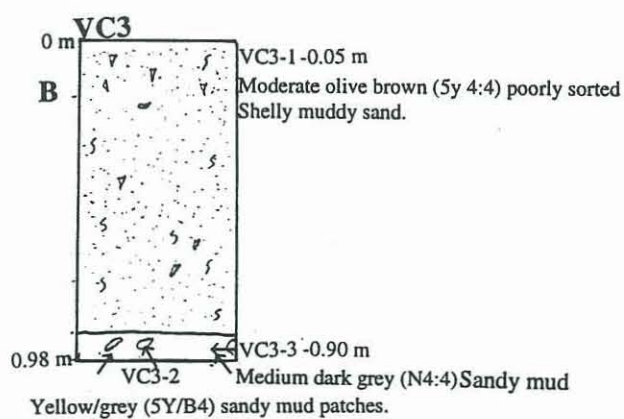


Figure 5.17. Data summary of vibrocore VC3 including: A) Graph of carbonate %; B) Vibrocore summary log of VC3; C) Grain size distribution of samples from VC3.

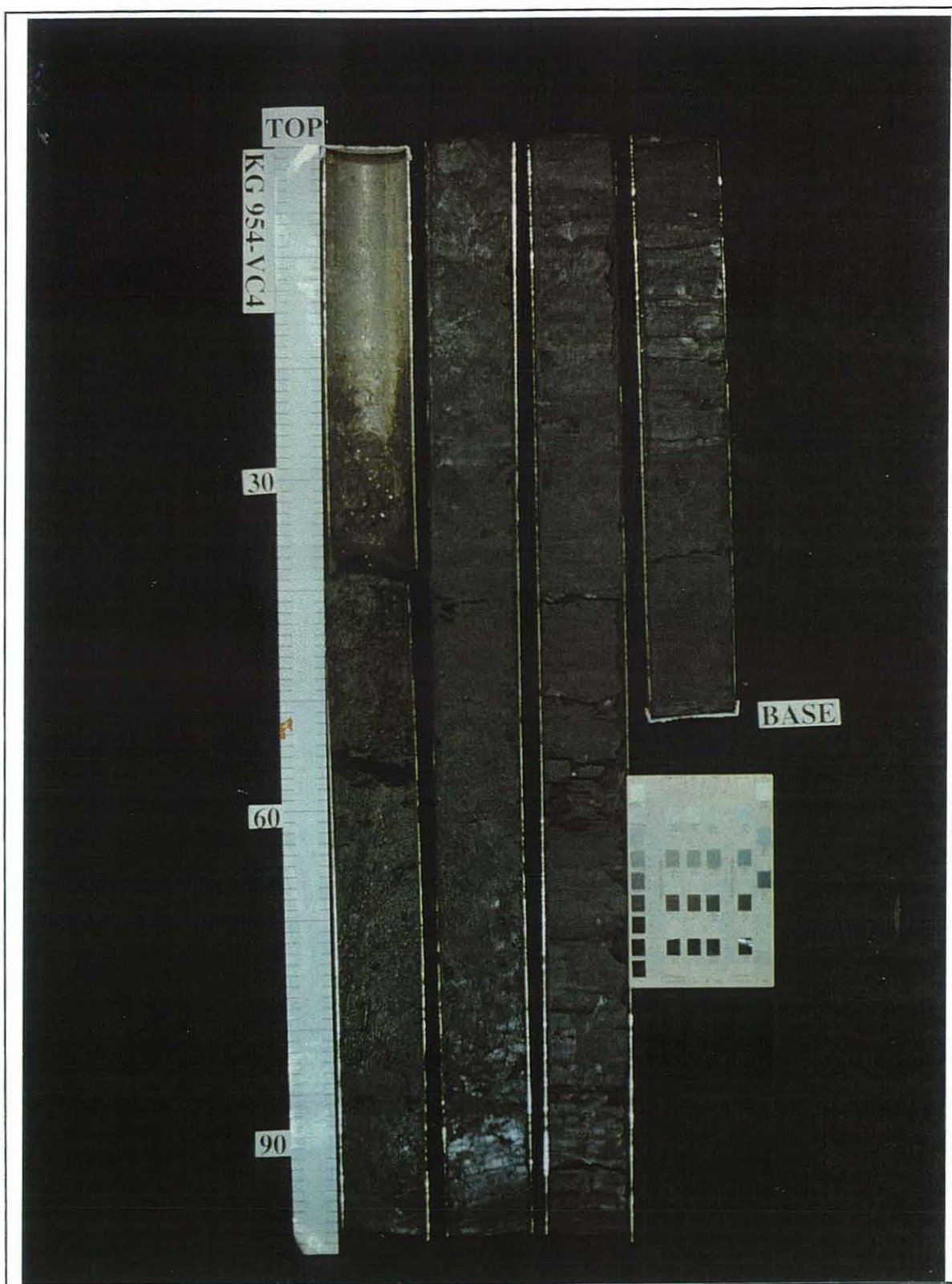


Figure 5.18. Vibrocore KG954-VC4. Facies include the bay fill (01.68 m) channel (1.68-2.90 m) and the mangrove facies (2.90-3.18 m).

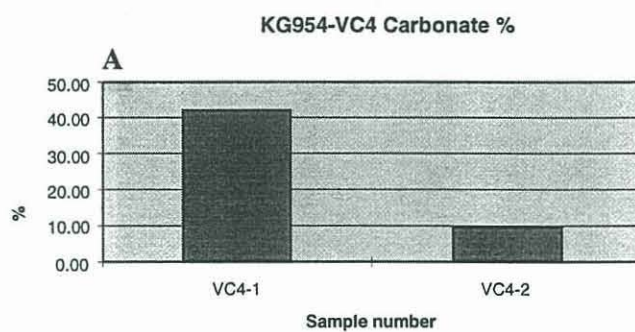
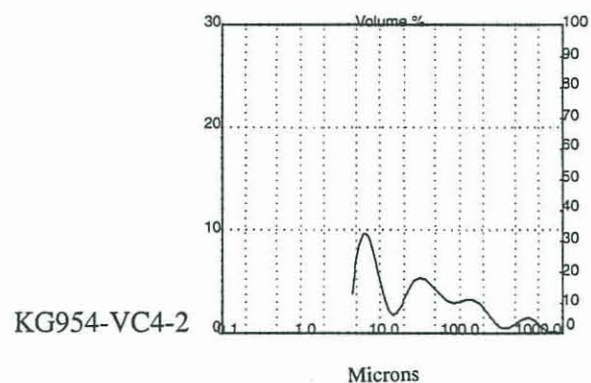
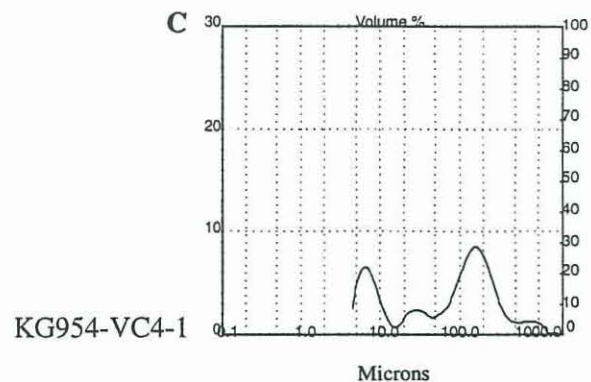
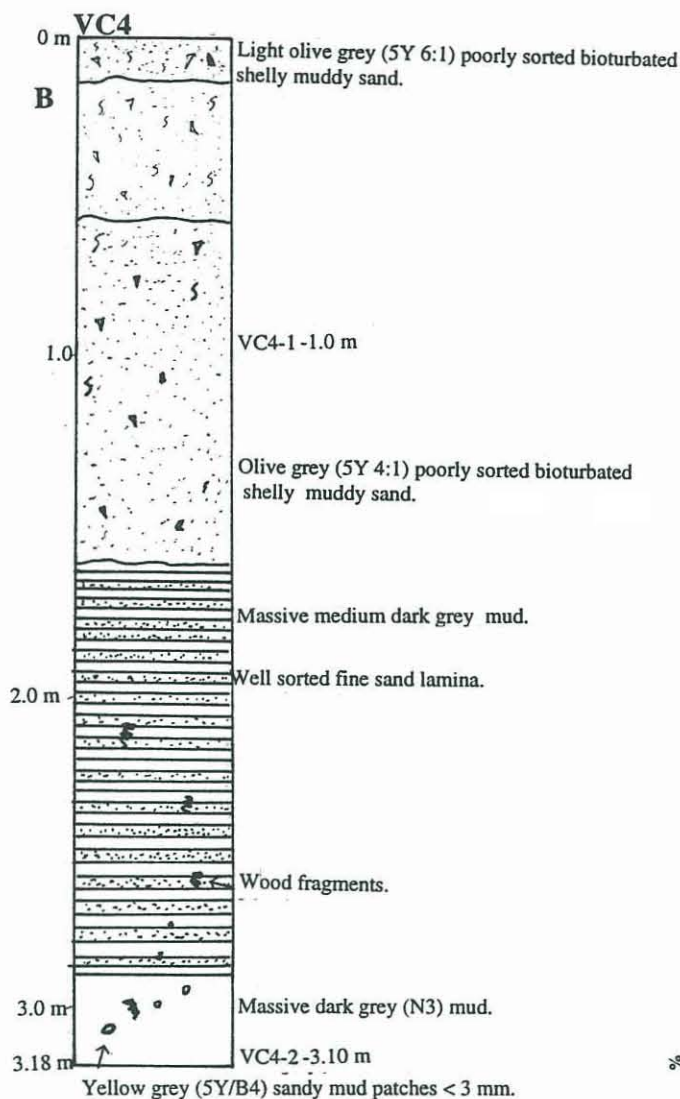


Figure 5.19. Data summary of vibrocore VC4 including: A) Graph of carbonate %; B) Vibrocore summary log of VC4; C) Grain size distribution of samples from VC4.

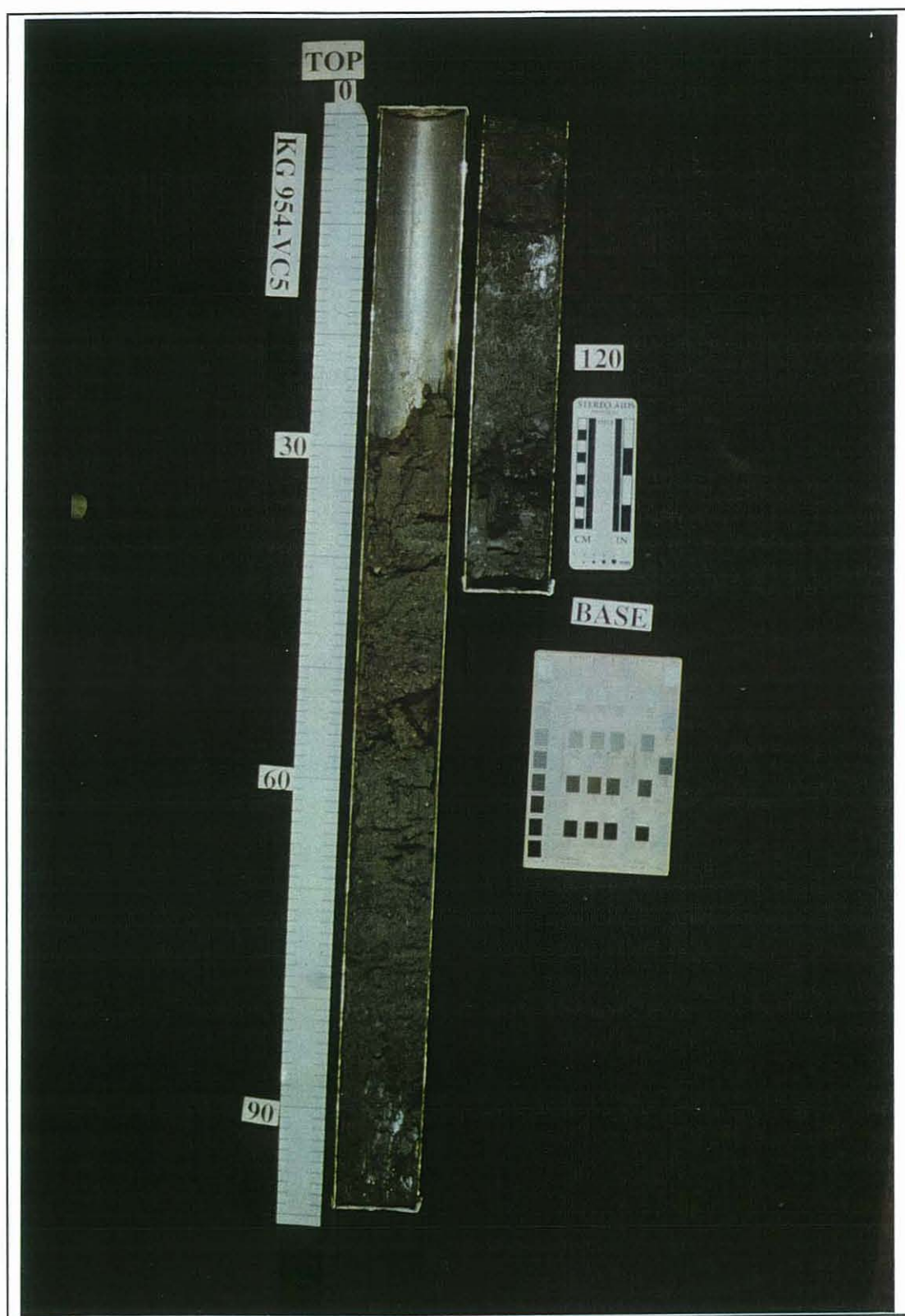


Figure 5.20. Vibrocore KG954-VC5. Facies include the bay fill (0-1.0 m) and the mud flat facies (1.0-1.12 m).

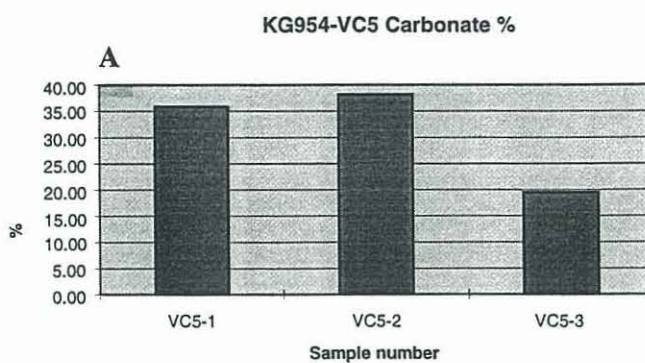
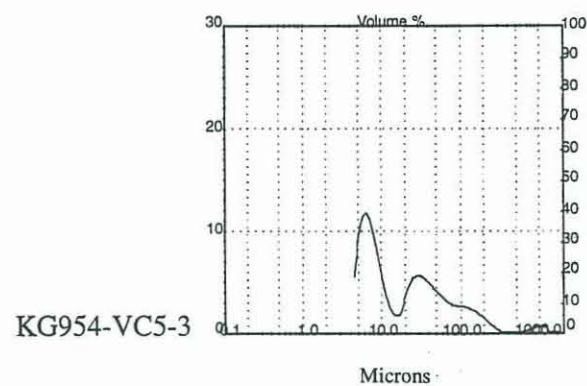
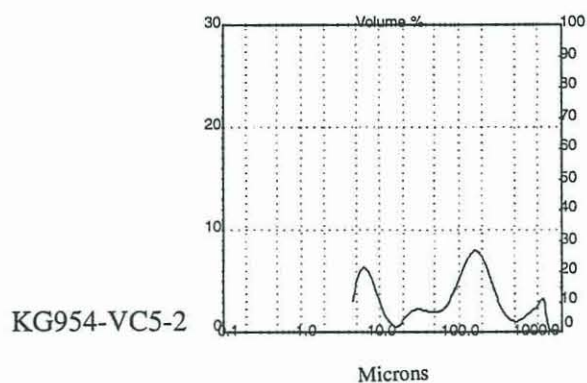
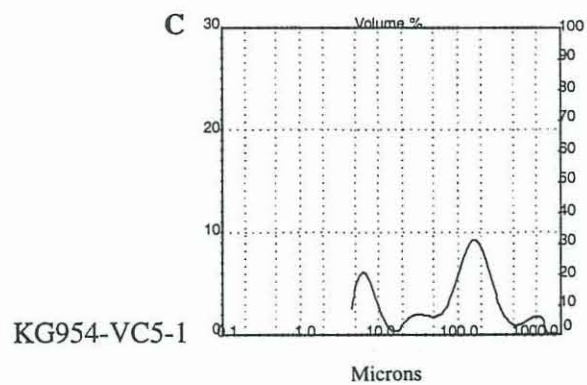
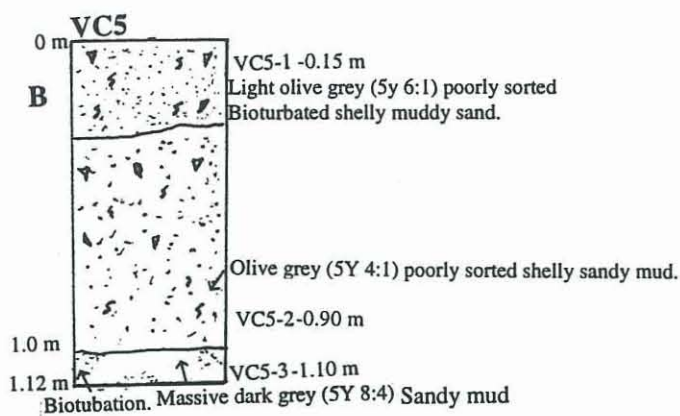


Figure 5.21. Data summary of vibrocore VC5 including: A) Graph of carbonate %; B) Vibrocore summary log of VC5; C) Grain size distribution of samples from VC5.

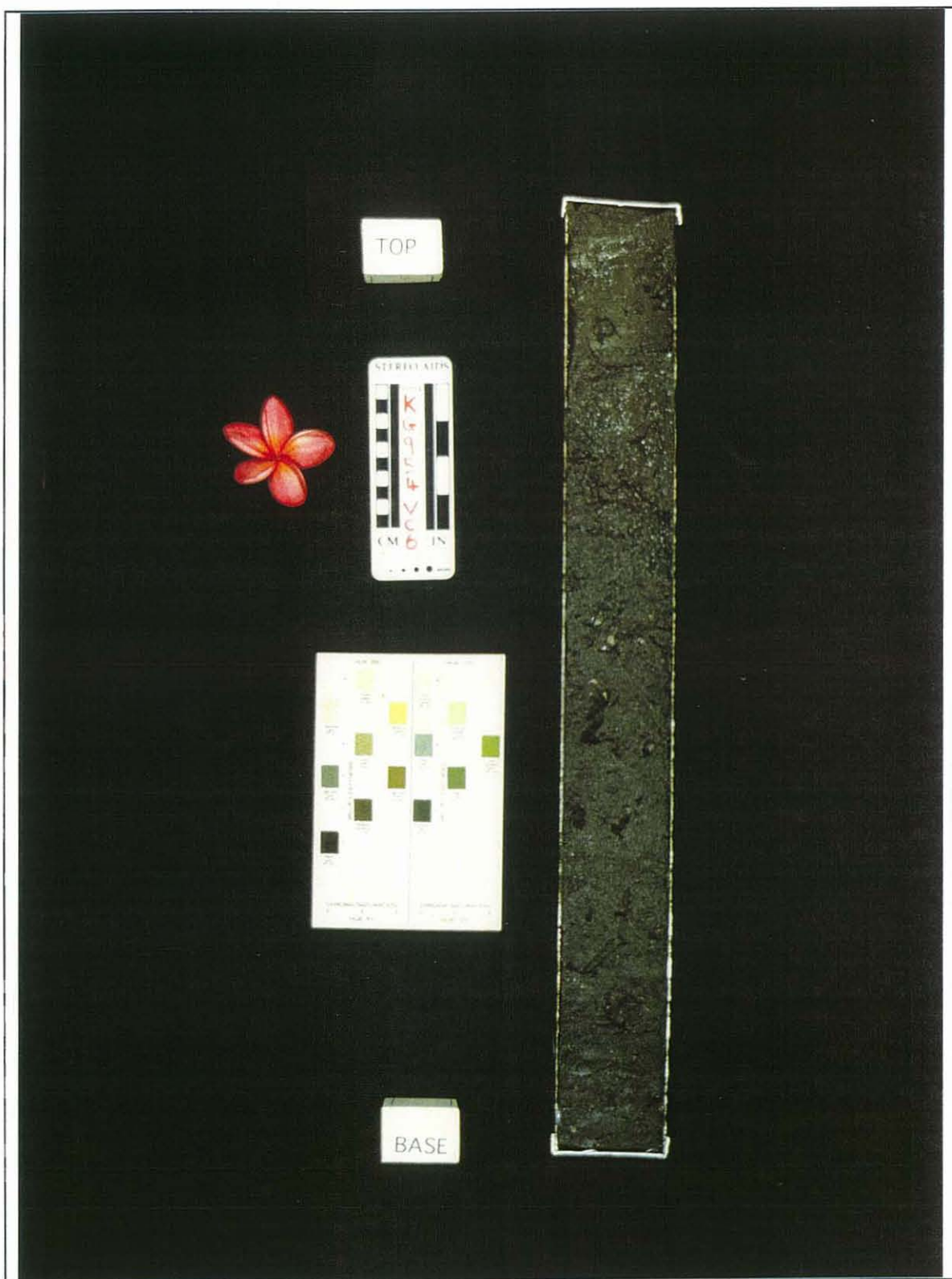


Figure 5.22. *Vibrocore KG954-VC6. Facies include the bay fill facies (0.-0.66 m).*

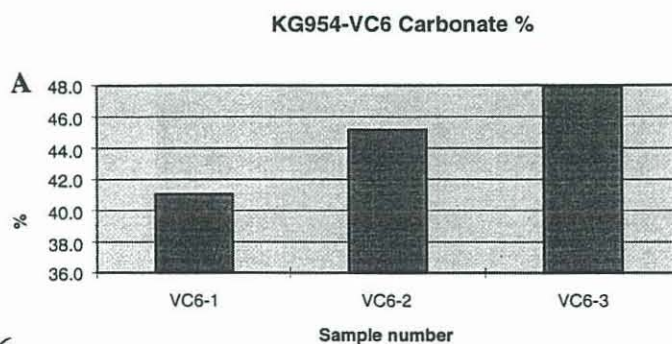
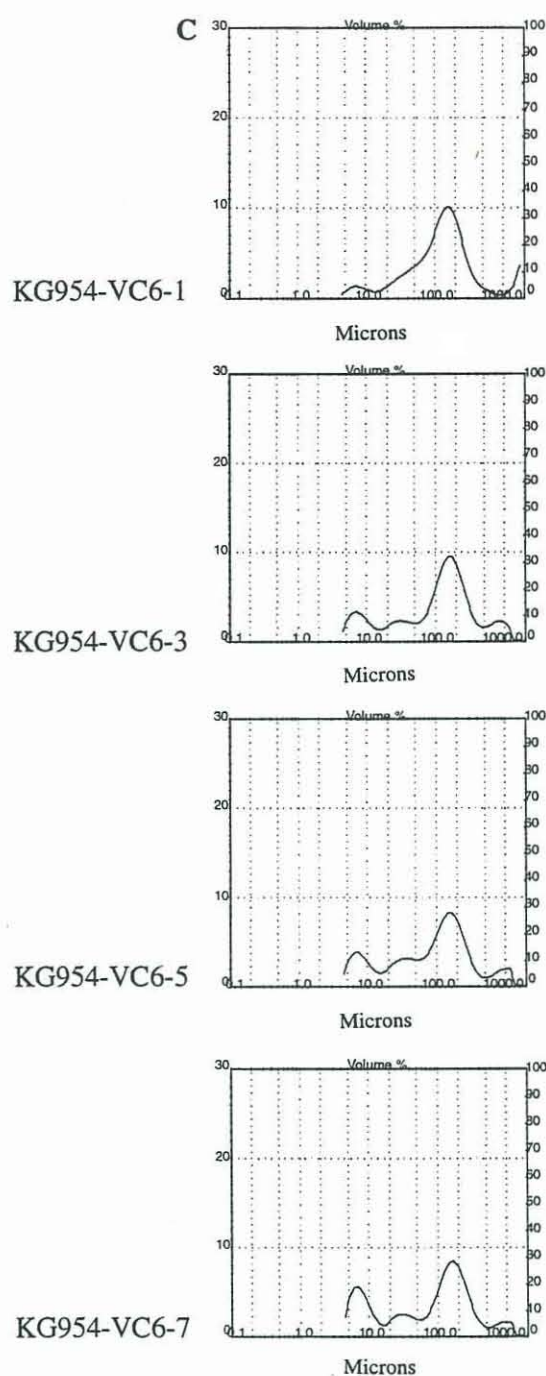
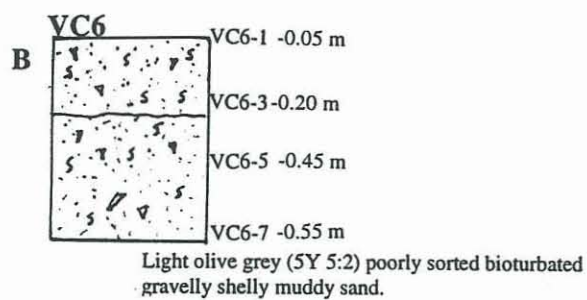


Figure .23. Data summary of vibrocore VC6 including: A) Graph of carbonate %; B) Vibrocore summary log of VC6; C) Grain size distribution of samples from VC6.

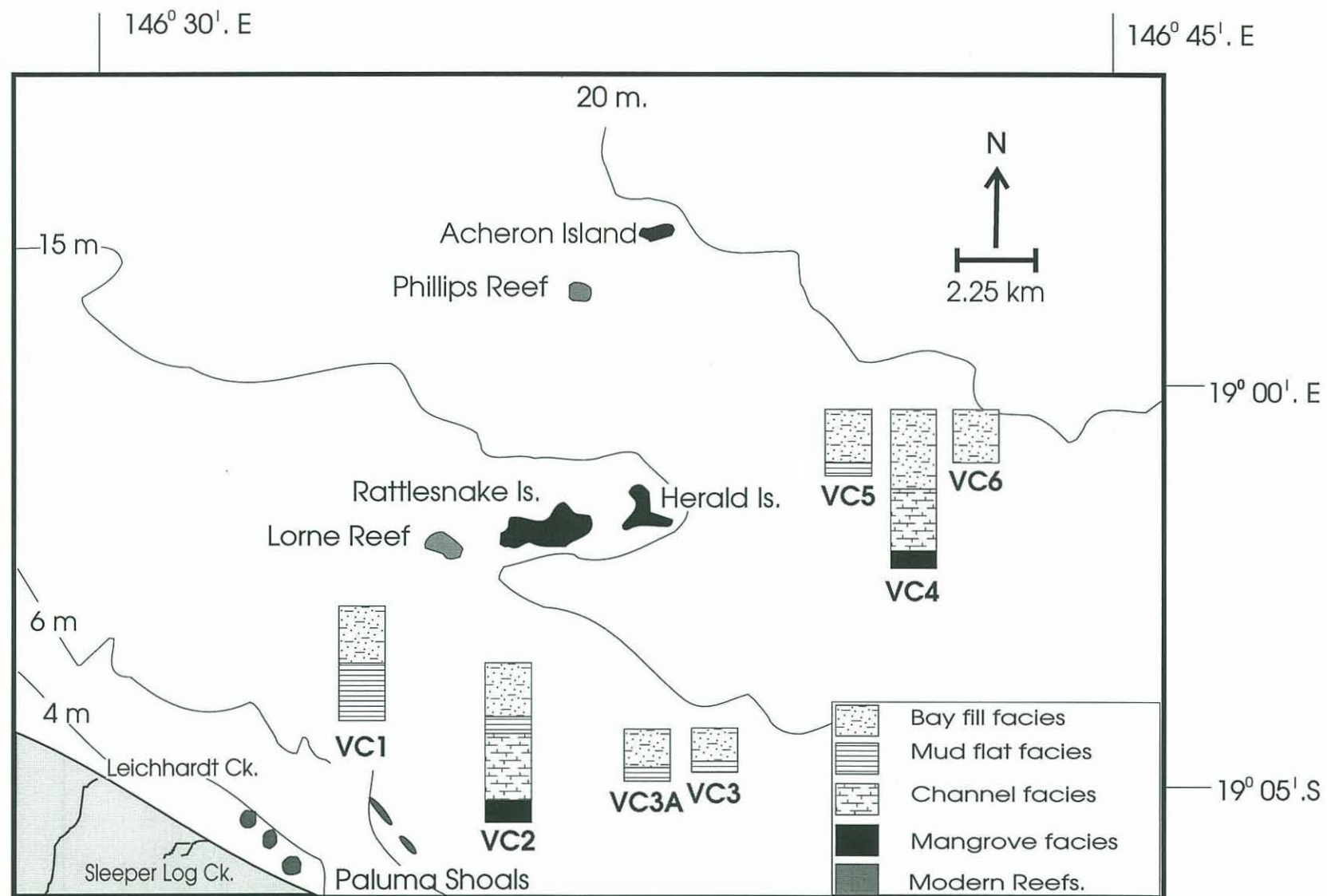


Figure 5.9. Summary vibrocore logs from southern Halifax Bay. The top of each core is plotted approximately in correct position, apart from VC3A which shares the same location as VC3. VC5 and VC6 also share the same position as VC4.

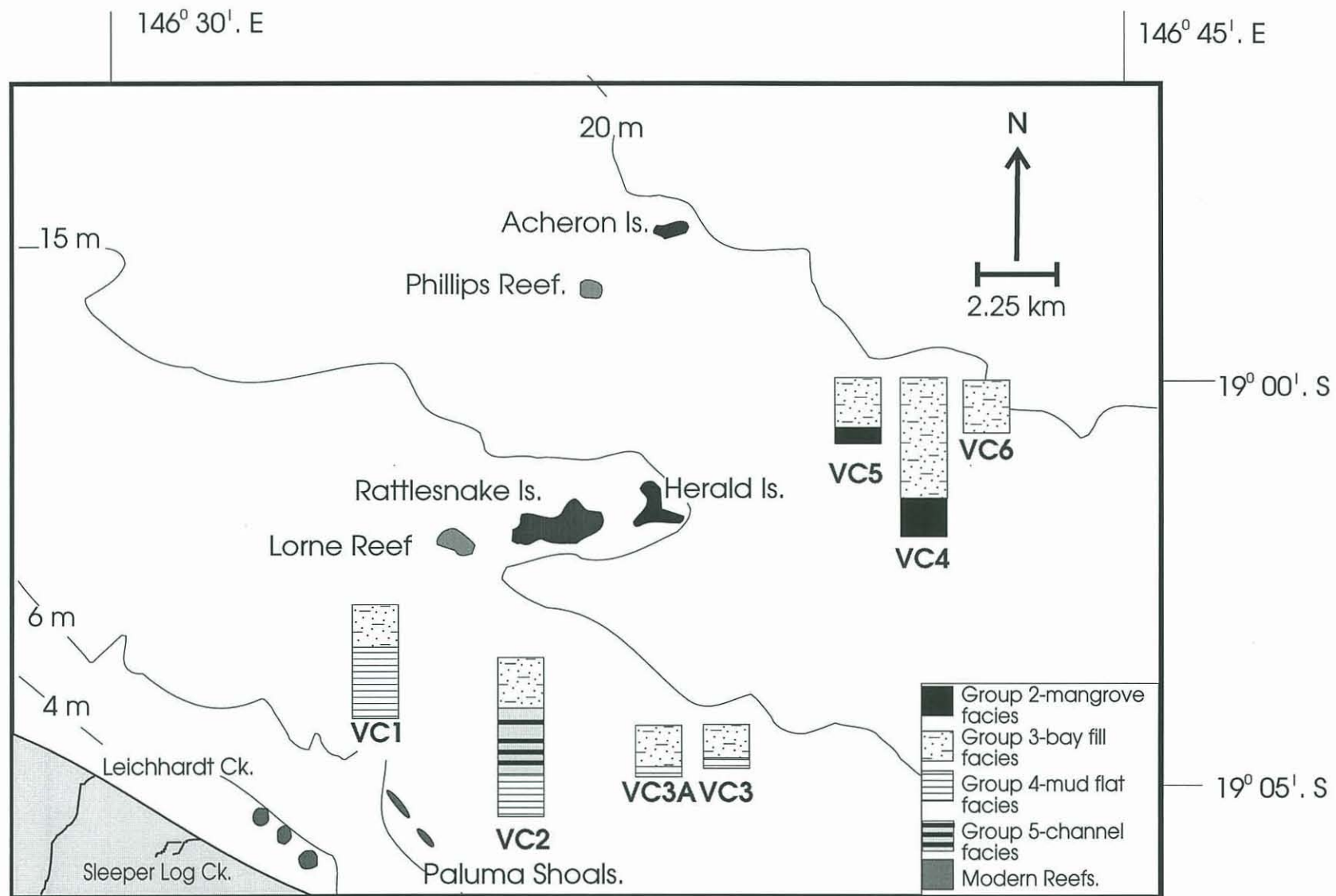


Figure 5.24. Entropy grouped facies in vibrocore VC1-VC6. The top of each core is plotted approximately in correct position. Entropy group boundaries are inferred however the groups compare well with the observed facies.